PERSISTENT LARGE-SCALE FLOW ANOMALIES. PART II: RELATIONSHIPS TO VARIATIONS IN EDDY ACTIVITY AND CYCLOGENESIS

Randall M. Dole

Center for Meteorology and Physical Oceanography, MIT
Cambridge, MA
U S A

Abstract

Observational analyses have been conducted to examine how changes in synoptic-scale eddy activity are related to changes in the large-scale flow that accompany persistent anomalies. We concentrate here mainly on identifying the relationships between variations in eddy activity and changes in the large-scale flow that occur between major cases of persistent positive and negative anomalies over the North Atlantic Ocean. The former cases are generally associated with blocking, while the latter are typically associated with anomalously intense zonal flows.

We focus first on identifying how synoptic-scale eddy activity varies for the widely differing large-scale flows. Spatial distributions of the root-mean-square variability of "band-pass" filtered sea-level pressure fluctuations for anomalous periods are compared with similar distributions obtained for the climatological-mean flow. The results show that the persistent anomalies are accompanied by pronounced changes in storm activity. Synoptic-scale variability is strongly suppressed in the vicinity of and immediately to the east of the blocking high, while enhanced variability occurs well northward of the mean storm path location. Strongly enhanced variability also occurs to the east of Greenland in the blocking cases, suggesting that in these cases orographic influences are also likely to play a significant role.

Next, contributions of the eddies toward maintaining local balances of heat, vorticity and potential vorticity are examined to study how changes in eddy activity may influence the large-scale flow anomalies. Comparisons between positive and negative cases show well-defined differences in most heat budget terms, but fewer significant differences in the vorticity and potential vorticity terms. Many of the systematic differences in the eddy terms appear qualitatively consistent with changes expected for baroclinic waves evolving on a spatially-varying mean flow. In addition, the results for the blocking cases suggest that feedbacks from the eddies onto the large-scale flow may play a significant role in enhancing the persistence of the anomalous flow patterns.

1. INTRODUCTION

In Part II, the basic problem that we wish to consider is that of identifying the relationships between variations in storm activity and persistent flow anomalies, that is: *how are changes in synoptic-scale eddy activity related to changes in the large-scale flow that accompany persistent anomalies?* As in Part I , we will address this first as an observational problem, and then discuss some theoretical implications.

It will be helpful in approaching this problem to consider it in two parts: first, what are the effects of changes in the large-scale flow on synoptic-scale eddy activity and, second, what are the effects of changes in synoptic-scale eddy activity on the large-scale flow? The first question is related to the problem of how large-scale flow variations influence the development and propagation characteristics of synoptic-scale disturbances, while the second is related to the problem of how feedbacks from the synoptic-scale eddies influence the large-scale flow anomalies. Although we will find this separation of problems to be operationally useful, it is important to keep in mind that the actual relationships between the eddies and the large scale flow are in general non-linear and, in addition, that subtle indirect effects of eddy-mean flow interactions may sometimes play quite significant roles. Consequently, interpreting observational results on the relationships between the eddies and the large-scale flow is often especially challenging.

2. A FEW PREVIOUS RESULTS

Although meteorologists have devoted considerable effort to understanding the climatological mean relationships between synoptic-scale transient eddies and the large-scale flow (for reviews of observational and theoretical studies see, respectively, Holopainen, 1983, and Hoskins, 1983), until relatively recently, there were few systematic attempts to analyze how *temporal variations* in synoptic-scale eddy activity are related to persistent anomalies of the large scale flow. There seems little doubt, however, that persistent anomalies are accompanied by pronounced changes in storm activity. Observational investigations of persistent phenomena such as blocking, for example, have often stressed the close relationship between variations in the large-scale flow and major changes in storm paths (and indeed, with respect to blocking, it might be argued that such a relationship should be considered as fundamental).

Perhaps the clearest indications of systematic variations in storm activity have been provided in synoptic and climatological studies of blocking (e.g, Berggren *et al.,* 1949; Rex, 1950a, b; 1951). Fig. 1 (from Petterssen, 1956) illustrates several of the most characteristic features. Fig. 1 displays the daily frontal positions over two 10-day periods prior to and following the establishment of blocking over the eastern Atlantic and western Europe (this is the same case that is analyzed in detail in the classic study of Bergrren *et al.,* 1949). During the 10-day period prior to the formation of blocking (Fig. 1a), the upper-level flow over the North Atlantic is nearly zonal. Synoptic-scale disturbances during this period propagate mainly eastward along a relatively narrow band across the North Atlantic, with a primary genesis region extending from over the southeastern United States through the western Atlantic. In contrast, following the development of blocking (Fig. 1b), there are two major storm paths located well to the north and well to the south of the initial storm path position. Frontal systems approaching the blocking region from the west appear to slow in their eastward progression and to elongate meridionally before splitting into the northern or southern

branches of the flow. During this period, new areas of cyclogenesis also appear to the east of Greenland as well as over the Mediterranean.

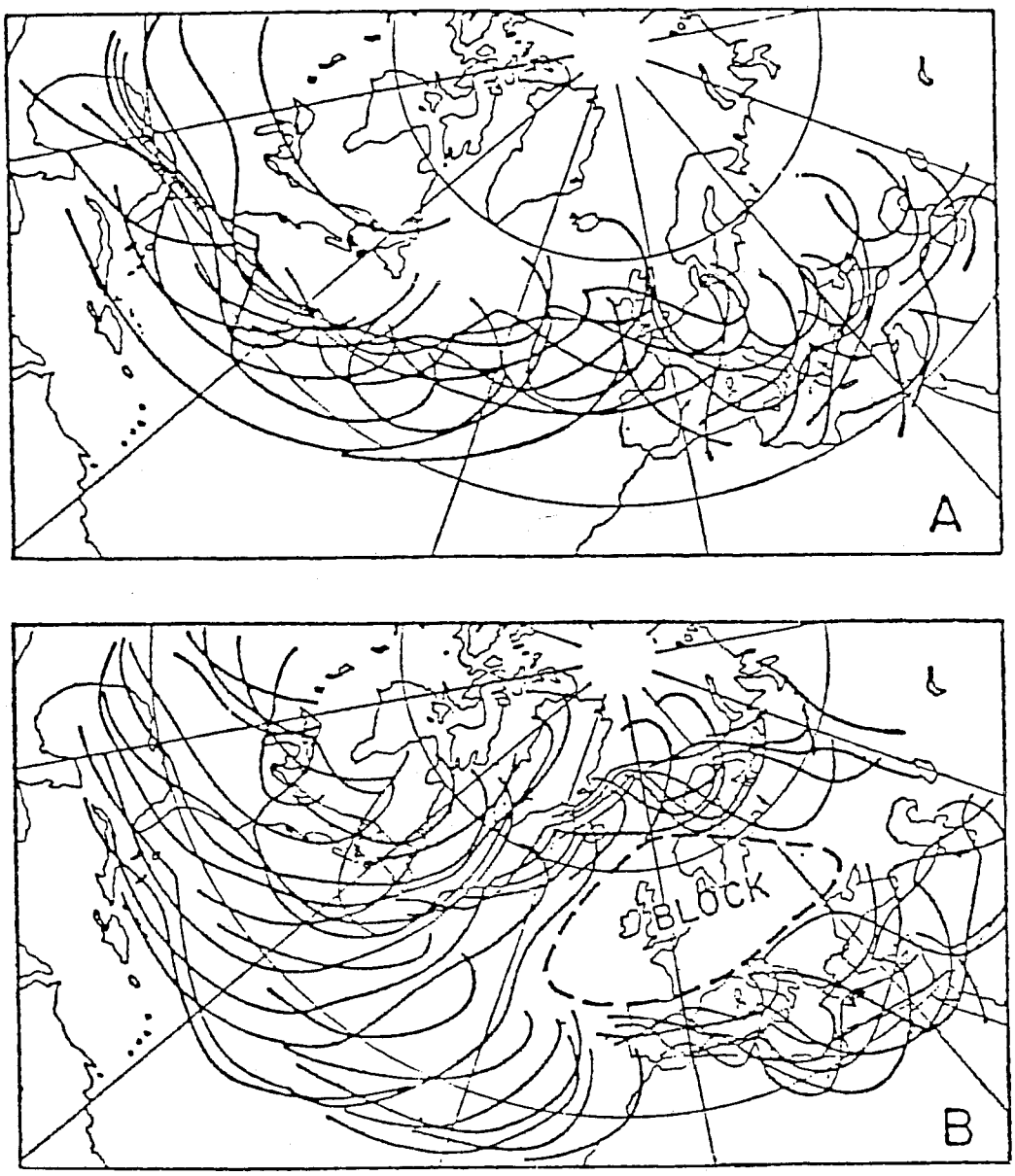

Fig. 1. Daily frontal positions during two successive 10-day periods : (a) preceding the formation and (b) following the development of blocking over the eastern Atlantic and western Europe (from Petterssen, 1956).

Most of the early studies stressed the apparent role of the large-scale anomalies in leading to the diplacements of storm paths from their mean locations. In recent years, there have been a number of simple theoretical studies that have demonstrated that the presence of a stationary planetary-scale wave can organize preferred regions for cyclogenesis in ways that seem broadly consistent with the early observations, although detailed comparisons for anomalous mean flows have not been made (Frederiksen, 1979; Niehaus, 1980; Pierrehumbert, 1986). Another major thrust of more recent observational and theoretical research has been toward understanding the influence of synoptic-scale eddies on the large-scale flow anomalies, particularly with respect to the question of whether forcing by synoptic-scale eddies may tend to enhance the persistence of the large-scale flow anomalies (e.g., Green, 1977; Austin, 1980; Hoskins *et al.*, 1983; Shutts, 1983; Illari and Marshall, 1983; Illari, 1984 ; Mullen, 1986; Trenberth, 1986a,b; Malanotte-Rizzoli and Malguzzi, 1987). In addition, several studies have also examined the problem of whether large-scale flow anomalies may be produced through nonlinear interactions between synoptic-scale eddies and planetary-scale waves (Egger, 1978; Gall *et al.*, 1979; Kalnay-Rivas and Merkine, 1981; Egger *et al.*, 1986; Shutts, 1986; Haines and Marshall, 1987; Metz, 1987). Although relatively fewer observational studies have focused on the latter problem, a number of cases have been described where intense synoptic-scale developments were apparently followed by the development of large-scale flow anomalies (e.g., Berggren *et al.*, 1949; Hansen and Chen, 1982; Sanders and Gyakum, 1980; Colucci, 1985, 1987). At this time, then, although there is considerable evidence that changes in synoptic-scale eddy activity and persistent flow anomalies are related, the extent and theoretical interpretation of the relationships remain uncertain.

3. EFFECTS OF LARGE-SCALE FLOW ON SYNOPTIC-SCALE EDDIES

Our initial objective will be to identify changes in synoptic-scale eddy activity that occur between periods characterized by widely-differing large scale flows. We will focus here primarily on identifying contemporaneous relationships at times when large-scale persistent anomaly patterns are fully developed. The basic data set and the procedures for selecting cases are as described in Part I. Case starting dates and durations, along with detailed descriptions of the composite time-average three-dimensional structures of the cases, are given elsewhere (Dole, 1982; Dole, 1986a).

3.1. Bandpass Variance Analyses

As an initial means for identifying changes in synoptic-scale eddy activity, we have determined the spatial distributions of the root-mean-square (rms) variability of "bandpass" filtered sea-level pressure fluctuations over various time periods, and have then compared the results obtained for anomalous periods with similar results obtained for the climatological-mean flow (Blackmon, 1976; Blackmon *et al.*, 1977). The "bandpass filter" used here retains periods in the range of approximately 2.5 - 6 days (for further details on this filter, see Blackmon, 1976). As shown by Blackmon *et al.* (1977), regions characterized by high bandpass variability are closely related to (although not identical with) the locations of the major storm paths. For brevity, we will adopt their (now commonly used) terminology and call the regions of maximum bandpass variance "storm paths".

For each 10-day period within the data set, we have first determined the field of the rms values of the bandpass sea-level pressure fluctuations; we will refer to these fields as the "10-day bandpass fields". The "climatological-mean" distribution of the 10-day bandpass fields, obtained by averaging over all of the 10-day periods in the data set, is shown in Fig. 2. As should be anticipated, this distribution is essentially identical to that of the

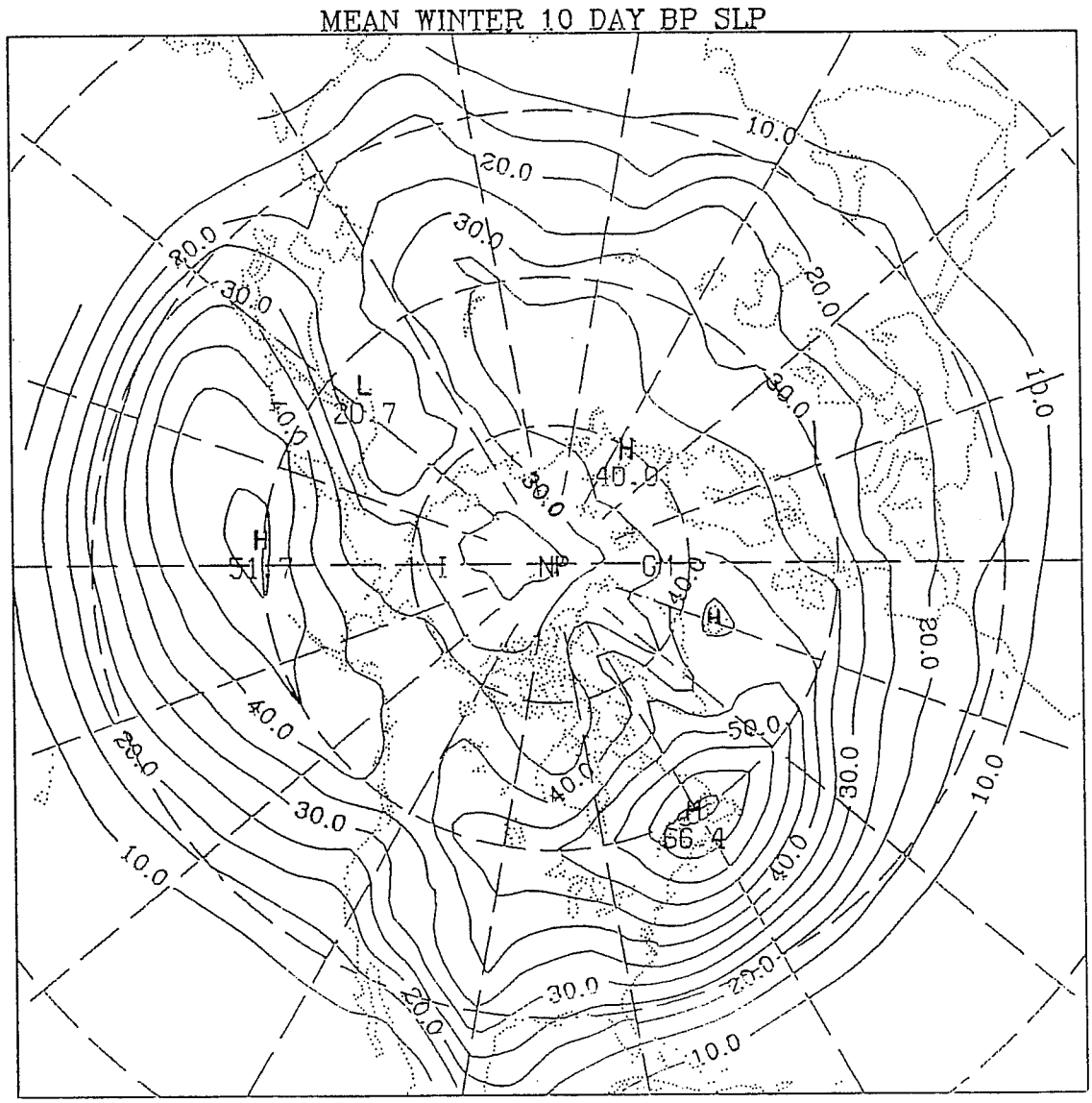

Fig. 2. The wintertime climatological-mean values of the rms variability in bandpass sea-level pressure fields occurring during 10-day periods (i.e., the average values of the "10-day bandpass fields"). Units: 10^{-1} mb.

climatological bandpass sea-level pressure variance described by Blackmon *et al.* (1977). The major regions of high bandpass variance, or "stormpaths", extend nearly zonally across the Atlantic and Pacific Oceans at mid-latitudes. In addition to the primary variance maxima located over the western North Atlantic near Newfoundland and over the west-central North Pacific slightly poleward and downstream of the major jet maxima, there are indications of weaker secondary maxima in bandpass variance over the northeastern Atlantic to the east of Greenland and over the northern Soviet Union.

Prior to examining the variability for particular anomalous periods, it will be useful to obtain some measure of the typical variability of the bandpass values between the different 10-day periods. One such measure of the "variability of the variability" can be obtained by determining the standard deviations of the 10-day values, as displayed in Fig. 3. We see that the largest standard deviations approximately coincide with the maxima in bandpass variance, suggesting that the largest variations about the mean values tend to occur near the regions of maximum storm activity. A measure of the *relative* "variability of the variability" can be obtained by dividing these standard deviations by their corresponding mean values, as shown in Fig. 4. We see that the relative variability of the bandpass fluctuations is not particularly large in the vicinity of the storm paths; indeed, the regions of smallest relative variability are located at mid-latitudes somewhat equatorward of the primary variance maxima. The greatest values of relative variability are mainly located either well poleward or well equatorward of the mean storm paths, regions where synoptic-scale eddy activity is typically rather low but in unusual synoptic situations (such as during blocking) may be greatly increased.

We have constructed composite analyses of 10-day bandpass anomalies for various times relative to the development of persistent anomalies, where the anomalies are defined as deviations of the 10-day bandpass fields from their local climatological average values (as shown in Fig. 2). As in Part I , composites were obtained by averaging over all

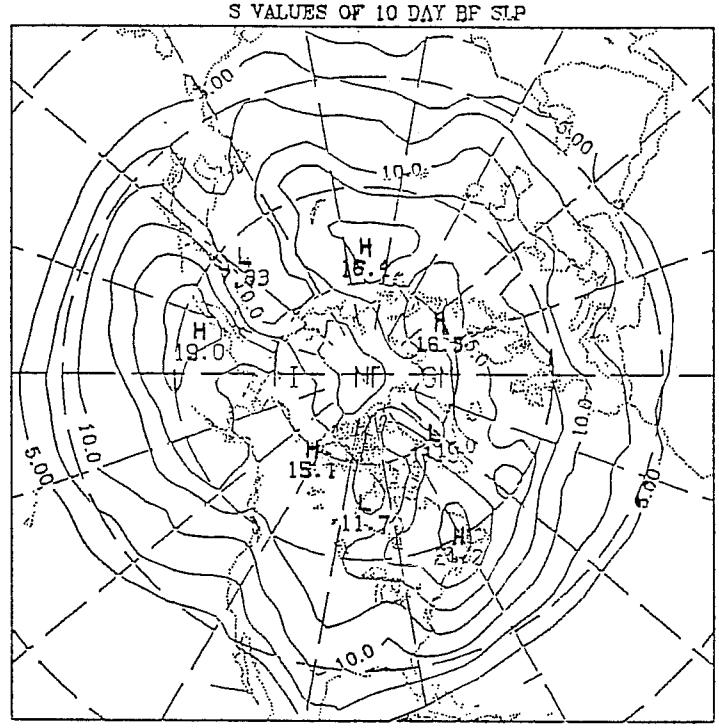

Fig. 3. The standard deviations of the 10-day bandpass fields about their climatological mean values. Units: 10^{-1} mb.

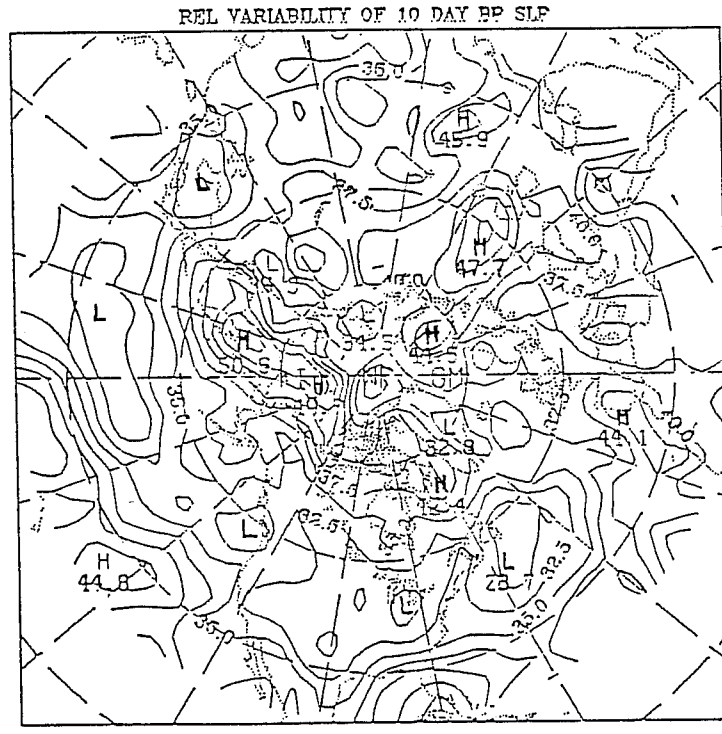

Fig. 4. The "relative" variability of the 10-day bandpass fields, obtained by normalizing the standard deviations displayed in Fig. 3 by the corresponding mean values shown in Fig. 2. Values are given in percent of the mean values.

corresponding cases relative to the start times; here, however, the compositing time refers to the center day in the averaging period (e.g., the 10-day bandpass composite for day + 6 is determined by the average of the case rms band-pass fields for the 10 day period from day + 1 to day + 11). In the following, we will primarily focus on times when the large-scale anomalies are around their maximum values.

Fig. 5 shows, for 15 persistent Pacific positive anomaly cases and for the same 14 Pacific negative anomaly cases analyzed in Part I, composite analyses of the 500 mb heights and sea-level pressure bandpass anomalies for the 10-day period centered on day + 6 . As the maximum 500 mb height anomalies occur at around this time, the differences between mean flows for the positive and negative cases are near their most extreme values.

The mean 500 mb flow for the positive cases (Fig. 5a) during this period is characterized by an anomalous ridge extending northward through the Aleutians, with mean troughs located near the western and eastern edges of the Pacific basin. Over the central North Pacific, the upper-level flow is diffluent and much weaker than normal. In several aspects, the basic pattern resembles that described by White and Clark (1975) in their analysis of blocking over the central Pacific. The corresponding bandpass anomalies (Fig. 5b) show strongly enhanced variability extending northeastward along the east coast of Asia to the Bering Sea; variability is also above normal to the east of the long wave trough over the northwestern United States, and in a region of enhanced zonal flow over the central United States to the lee of the Rockies. In contrast, variability is strongly suppressed over much of the central and eastern Pacific to the east of the anomalous upper-level ridge.

In the negative cases, the principal features of the 500 mb heights (Fig. 5c) are an intense upper-level vortex centered over the Aleutians that is associated with an abnormally strong jet across most of the Pacific, a highly amplified ridge near the west coast of the North America, and an abnormally deep long wave trough over eastern North America. The corresponding

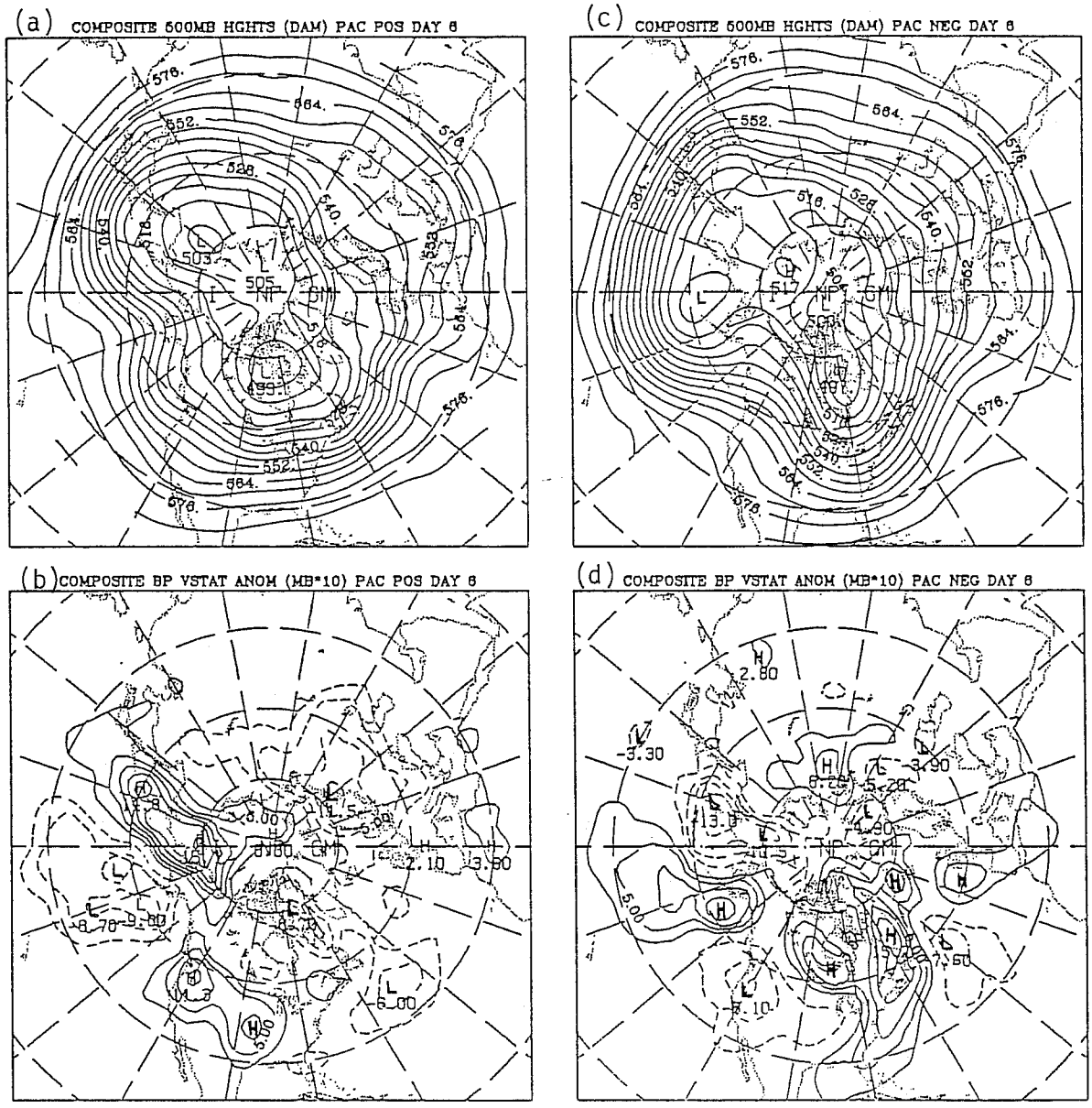

Fig. 5. (a) Composite 500 mb heights (units: dam) for 15 PAC positive anomaly cases for the 10-day period centered on day + 6. (b) The values of the composite anomalies in the 10-day bandpass sea-level pressure fields for the same PAC positive cases for the 10 days centered on day + 6 (units: 10^{-1} mb). (c) Composite 500 mb heights (units: dam) for 14 PAC negative anomaly cases for the 10-day period centered on day + 6. (d) The values of the composite anomalies in the 10-day bandpass sea-level pressure fields for the same PAC negative anomaly cases for the 10 days centered on day + 6 (units: 10^{-1} mb).

10-day bandpass anomalies (Fig. 5d) display three primary regions of enhanced eddy activity: the first extending from over the east-central North Pacific northeastward into the Gulf of Alaska, the second beginning on the lee side of the Canadian Rockies over Alberta, and the third located near the east coast of North America to the east of the major long wave trough axis. Conversely, eddy activity is strongly suppressed in the far northwest Pacific in the region of weak flow far to the north of the major baroclinic zone and over the western United States near and to the east of the major upper-level ridge.

In both positive and negative anomaly cases, the patterns of the bandpass anomalies broadly conform with synoptic experience. Enhanced variability tends to occur near and to the east side of the major long wave troughs (as near the east coast of North America in the negative anomaly cases), and on the lee side of mountains in regions of stronger than normal flow (as to the east of the U.S. Rockies in the positive cases and to the east of the Canadian Rockies in the negative cases). Conversely, variability is usually strongly suppressed near and to the east of major long wave ridges (as over the central Pacific in the positive cases and over the western United States in the negative cases).

Fig. 6 shows similar analyses conducted for 12 positive anomaly and 12 negative anomaly cases located instead over the eastern North Atlantic (the ATL cases). The ATL positive cases (Fig 6a) are associated with a highly amplified ridge and split flow over the eastern North Atlantic, with one branch of westerlies to the north of the ridge and a weaker second branch located far to the south. This flow configuration is reminiscent of the Atlantic blocking patterns described in the classic studies by Rex (1950a,b), although the primary anticyclonic centers in his cases were typically displaced somewhat further northeastward toward Scandanavia. Variability in these cases (Fig. 6b) is enhanced well upstream of the ridge over eastern Canada and the northwest Atlantic extending toward Baffin Island, and from the lee side of Greenland southeastward toward the Caspian Sea. In contrast, variability is strongly suppressed over most of the North Atlantic near and downstream from

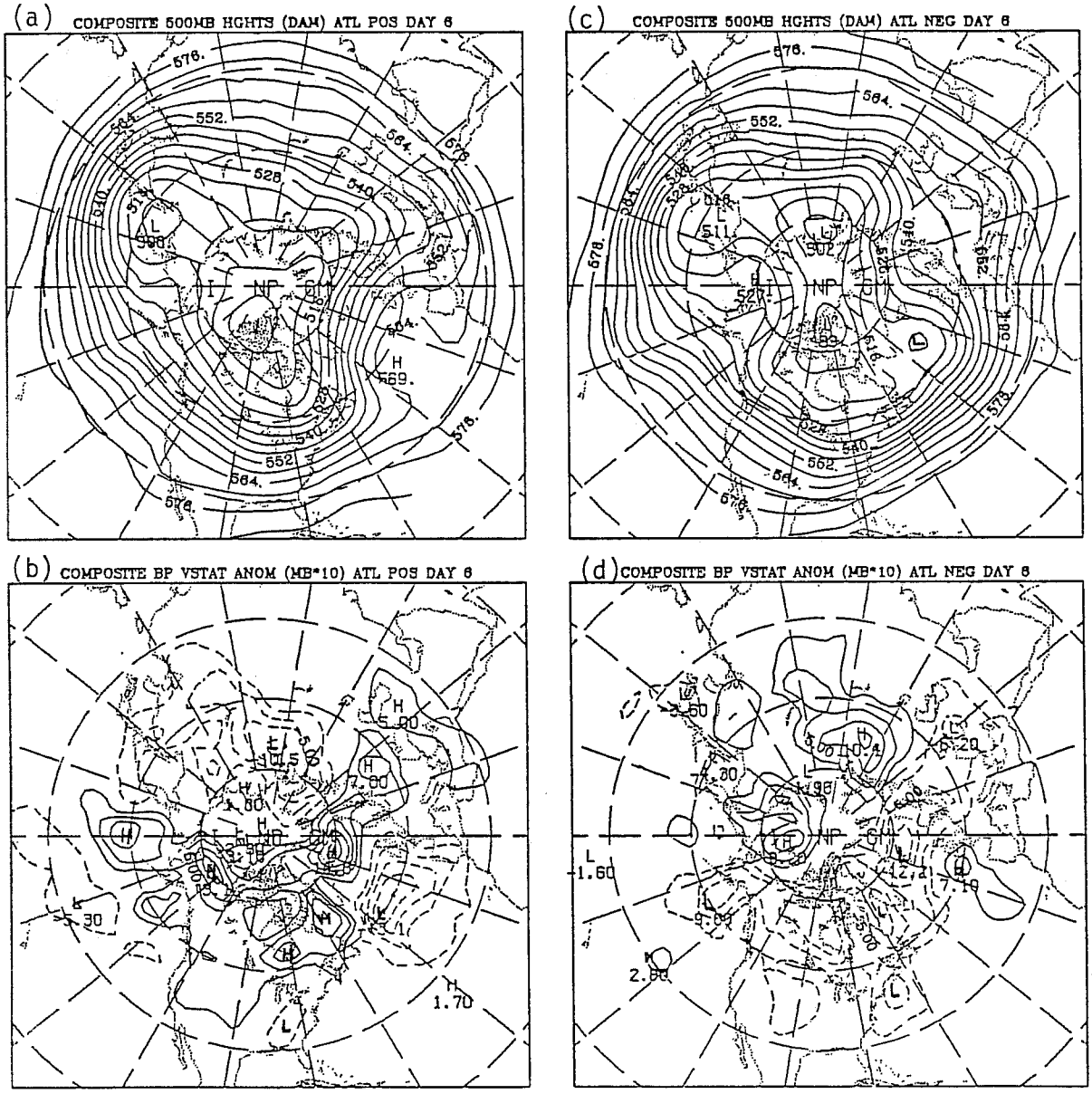

Fig. 6. (a) Composite 500 mb heights (units: dam) for 12 ATL positive anomaly cases for the 10-day period centered on day + 6. (b) The values of the composite anomalies in the 10-day bandpass sea-level pressure fields for the same ATL positive cases for the 10 days centered on day + 6 (units: 10^{-1} mb). (c) Composite 500 mb heights (units: dam) for 12 ATL negative anomaly cases for the 10-day period centered on day + 6. (d) The values of the composite anomalies in the 10-day bandpass sea-level pressure fields for the same ATL negative anomaly cases for the 10 days centered on day + 6 (units: 10^{-1} mb).

the ridge axis. The ATL negative cases (Fig. 6c) are characterized by an anomalously strong and southeastward-displaced Icelandic low with a single, intense westerly jet extending across most of the North Atlantic. Variability in these cases is suppressed over most of the North Atlantic, with the exception of a small region over the extreme eastern Atlantic that is located on the east side of the long wave trough axis.

As in the time-mean anomaly fields, the large-scale patterns of the bandpass anomalies for corresponding positive and negative cases display a number of striking similarities, so that to a first approximation, the sign of the bandpass anomalies also tends to reverse when comparing the positive and negative cases for a given region. This tendency toward symmetry in the bandpass anomalies can be evaluated more readily by taking the differences between corresponding fields, as shown in Fig. 7.

For the PAC cases (Fig. 7a), we see that, relative to the negative cases, the positive cases show considerably enhanced variability from along the east coast of Asia northward toward the Bering Sea, and from over the extreme eastern Pacific southeastward toward the western Plains of the United States. Conversely, the bandpass variability for the positive cases is considerably lower than the negative cases from over the central North Pacific northeastward into southern Alaska, along the east coast of North America northward to Baffin Bay, and to the east of the Canadian Rockies. For the ATL cases (Fig. 7b), bandpass variability in the positive cases is most enhanced relative to the negative cases over much of northern Canada, over the far northwest Atlantic to Baffin Bay, and over the northeast Atlantic from just east of Greenland southeastward through Scandanavia toward the western Soviet Union. Regions of relatively lower variability in the positive cases include much of the central and eastern North Atlantic and from the northern Soviet Union southeastward toward China. For both regions, then, pronounced differences are apparent in the locations of the storm paths between positive and negative anomaly cases. The observed changes are consistent with the general concept that blocking is associated with major shifts in the regional storm paths.

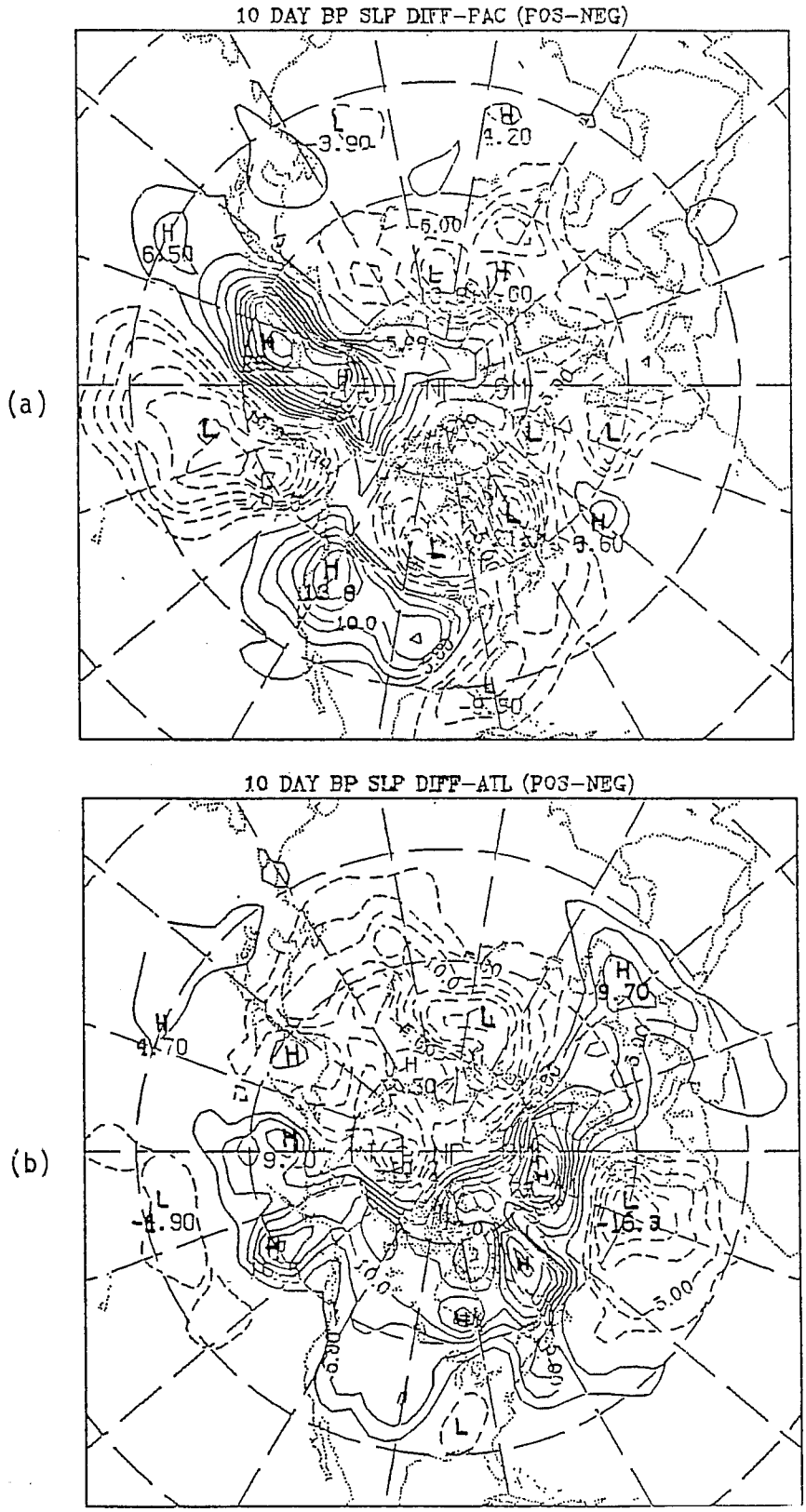

Fig. 7. Differences between the positive and negative cases in the composite 10-day bandpass sea-level pressure fields (positive - negative) for the 10-day period centered on day + 6. (a) PAC cases. (b) ATL cases.

3.2. Variations in Cyclogenesis Associated With Persistent Temperature Anomalies

We are currently conducting some parallel studies on persistent anomalies in surface temperatures. We will briefly discuss a few early results of this research that suggest that there are also significant variations in cyclogenesis associated with the persistent temperature anomalies.

In a pilot study on this project, Mr. Brad Lyon of MIT has studied variations in cyclogenesis occurring in association with wintertime cases of persistent temperature anomalies at Boston, MA (which, in winter, is located just on the northwest side of the zone of maximum time-mean baroclinity). There were 8 warm and 10 cold events selected for study, with average temperature departures and durations for the events being $\pm 10^{o}$ F and 10 days. For all cyclones observed during the events within the region between 25^{o} N - 60^{o} N and 120^{o} W - 40^{o} W, the 24 h intensification rates and total central pressure falls were determined (a total of 56 cyclones for the warm cases and 60 cyclones for the cold cases).

Fig. 8a shows for both the warm and cold cases the distributions of maximum 24 hr deepening rates observed for all cyclones. The warm cases display a relatively strong peak at around 11 mb / 24 hr , with only a few cases showing relatively rapid deepening rates. In contrast, in the cold cases, the distribution of deepening rates is substantially broader and has higher mean and modal values, with far more cases undergoing rapid deepening. By the conventional criterion for defining explosive cyclogenesis (Sanders and Gyakum, 1980), in the warm cases only 3 cyclones underwent explosive deepening, while in the cold cases there were 18 cases of explosive cyclogenesis.

Fig. 8b displays the total central pressure falls occurring during periods characterized by

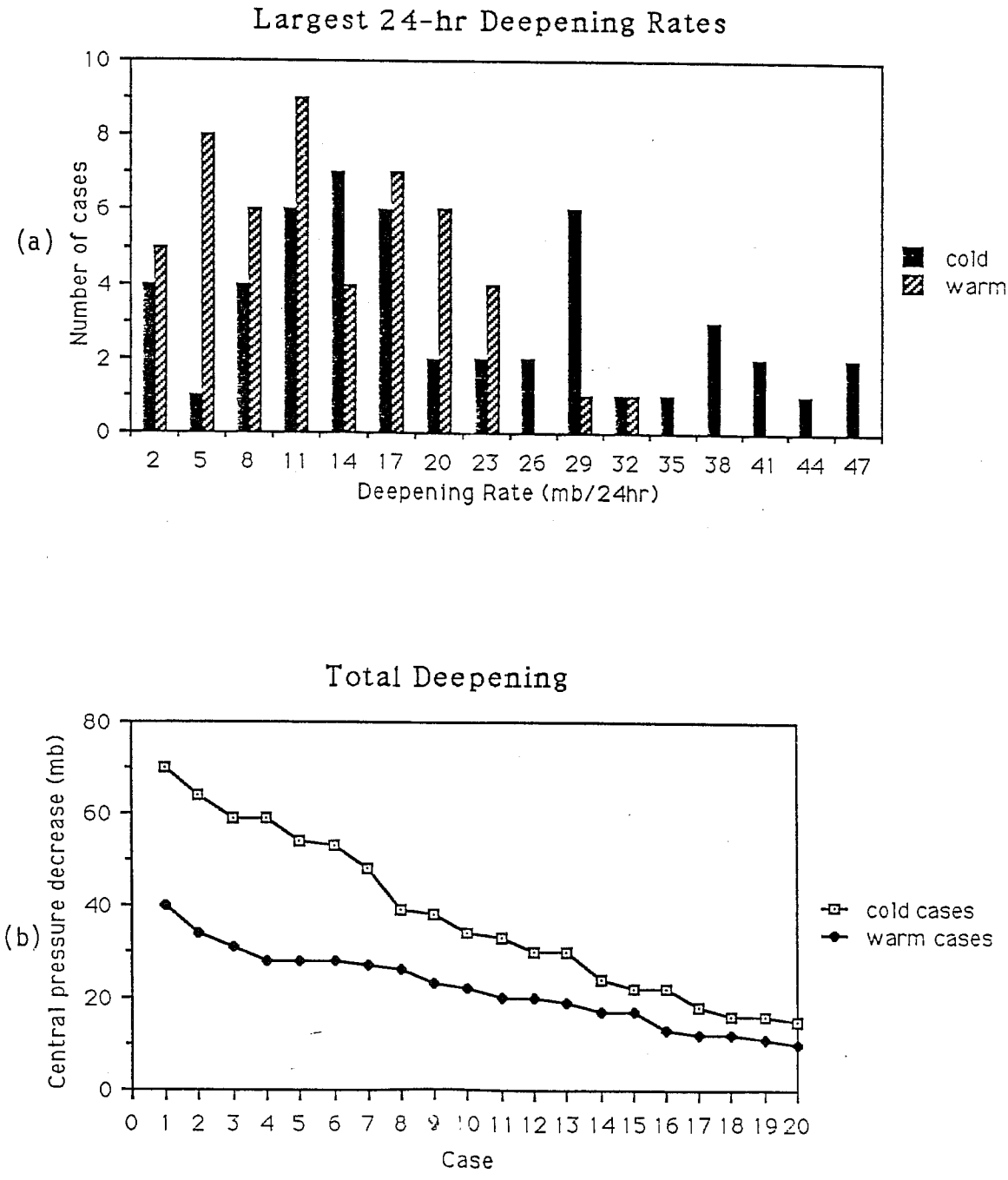

Fig. 8. (a) Maximum 24 h pressure falls for cyclones during warm events and cold events (units: mb) . (b) Total central pressure falls for the 20 cyclones in both warm cases and cold cases undergoing the greatest total deepening (units: mb).

continuous deepening for the 20 cyclones in both the warm and cold cases that underwent the greatest total deepening. In general, the total pressure falls during development were considerably larger in the cold than in the warm cases so that, compared with cyclones observed in the warm events, cyclones observed in the cold events typically underwent not only more rapid deepening, but also a greater total deepening. Additional results (not shown) indicate that there are also significant changes in the geographical distribution of cyclogenesis associated with the persistent temperature anomalies, with a tendency for cyclogenesis to be relatively more common over land in the warm cases and over the oceans in the cold cases.

We believe that, although these results are preliminary, the general differences in cyclogenesis between warm and cold events described here will be confirmed in more extensive studies. Although some of the differences in cyclogenesis are likely to be attributable to variations in the mean long wave patterns between the persistent warm and cold events, it seems plausible to us that the effects of variations in surface baroclinity and in static stability (particularly in the lower troposphere) are also likely to be quite significant.

4. EFFECTS OF SYNOPTIC-SCALE EDDIES ON LARGE-SCALE FLOW

We now turn to the problem of how feedbacks from the synoptic-scale eddies influence the large-scale flow. The analysis of the effects of eddies on mean flows is a difficult and subtle problem that in recent years has been the subject of a great number of both theoretical and observational studies. In this section, we will focus first on a few results obtained from time-mean budget studies, and then briefly examine more recent alternative methods that have been developed for diagnosing the effects of eddies on mean flows.

4.1. Time-mean budget studies

The basic approach adopted in the budget analyses is as follows. First, time-mean budgets of heat, vorticity and potential vorticity are calculated for persistent anomaly cases in a given region. From the case-mean results, ensemble averages are then constructed for both positive and negative anomaly cases by averaging over all cases of like sign. The contributions by the various terms to the time-mean balances are then compared to ascertain whether the observed differences between positive and negative anomaly cases are statistically significant.

Before examining results for anomalous mean flows, it is useful to recall a few of the basic results obtained for climatological-mean conditions. From numerous observational, theoretical and modelling studies of the behavior of synoptic-scale eddies in the climatological-mean flow (e.g., Blackmon *et al.*, 1977; Lau, 1978, 1979a; Holopainen, 1983; Hoskins, 1983; Held and Hoskins, 1985), the general picture that has emerged is that eddy activity initially increases at low-levels at the start of the major storm paths over the eastern continent - western ocean regions and grows baroclinically while propagating upwards and eastwards. At the downstream end of the storm paths over the central oceans, eddy activity propagates mainly horizontally, with the energy propagation being

predominantly equatorward. Particularly at the start of the storm paths, there are strong downgradient heat fluxes that have peak values in the lower troposphere, with a convergence of westerly momentum flux into the storm path regions that is largest at upper levels. At the downstream end of the storm paths, the equatorward energy propagation is associated with a strong poleward momentum flux, with maximum flux convergence on the poleward side of the mean jet axis.

On the basis of these analyses, the mean flow tendencies resulting from the direct effects of the eddies appear to be toward decreasing the vertical shear (reducing the baroclinity) and increasing the barotropic component of the flow (in particular, increasing the surface westerlies), and in addition, shifting the mean jet axis poleward, particularly in the jet exit regions. As we will discuss, however, inferring the effects of the eddies on the mean flow from the tendencies due to the observed eddy fluxes can be misleading; Held and Hoskins (1985) provide some interesting illustrations of potential difficulties.

In the following, we will focus mainly on differences in eddy terms obtained for cases having persistent anomalies over the central North Atlantic (ATL cases) ; more complete descriptions of the budget results are given in Dole (1982). Composite analyses were derived from 12 ATL positive cases (total durations of 196 days) and 12 ATL negative cases (total durations of 213 days). Dole (1986) provides starting dates and durations of the cases, along with more detailed descriptions of their time-mean structures and bandpass variance characteristics.

4.1.1. Differences in time-mean fields and storm paths

In interpreting the results of the time-mean budget calculations, it will be helpful to have descriptions of the corresponding mean height, temperature and vorticity patterns for these cases. Fig. 9 displays the time-mean 500 mb height patterns for the ATL cases; the

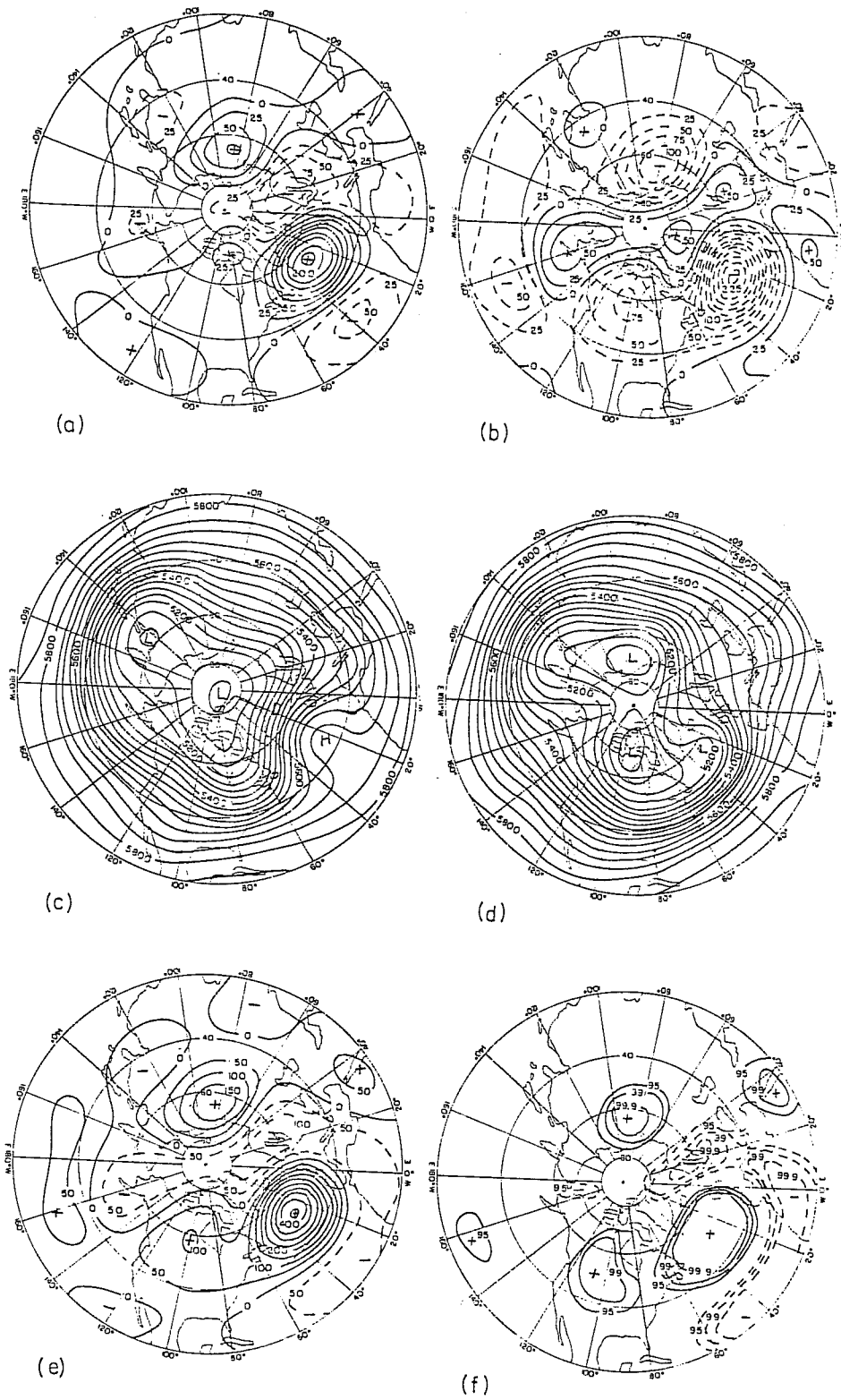

Fig. 9. (a) Composite 500 mb height anomalies (units: m) for (a) 12 ATL positive cases and (b) 12 ATL negative cases. Composite 500 mb heights (units: m) for the (c) positive cases and (d) negative cases. (e) (Positive - negative) 500 mb height differences (units: m); and (f) confidence levels for a two-sided t - test for the differences between means. Solid lines are positive differences as shown in (e), dashed lines are where the differences are negative.

corresponding 700 mb temperature patterns and 300 mb vorticity patterns are shown in Figs. 10 and 11.

To a first approximation, the 500 mb height anomaly patterns for the positive cases (Fig. 9a) and negative cases (Fig. 9b) appear as opposite phases of a single pattern that rather strongly resembles the Eastern Atlantic (EA) teleconnection pattern (Wallace and Gutzler, 1981). The positive cases, which are frequently associated with persistent blocking over the Atlantic, have a mean 500 mb height pattern (Fig. 9c) that is characterized by a strongly amplified ridge and split flow over the eastern Atlantic, with one branch of westerlies located to the north of the ridge and a weaker second branch located far to the south. In contrast, the negative cases (Fig. 9d) are associated with an abnormally strong zonal flow that extends across most of the Atlantic Ocean at mid-latitudes. Mean 500 mb height differences between the positive and negative cases (Fig. 9e) exceed 400 m over the eastern North Atlantic. As estimated from a two-sided t-test (null hypothesis of no difference between means), the differences in means are highly significant (Fig. 9f) over a large portion of the North Atlantic, over parts of Scandanavia, Europe and the Soviet Union in association with a downstream "wavetrain" pattern, and over north-central Canada and a small region near the Red Sea.

Comparing the 700 mb mean temperature analyses (Fig. 10) with the corresponding 500 mb height analyses, we see that (as throughout the troposphere) the positive height anomalies are predominantly warm-core and the negative anomalies cold-core, with the ATL temperature anomaly centers displaced just slightly westward of the corresponding 500 mb height maxima. In the positive cases (Fig. 10c), the strongest temperature gradients extend in a band from near Nova Scotia northeastward just to the south of Greenland and then eastward through Iceland. In contrast, the strongest gradients in the negative anomaly cases (Fig. 10d) occur from eastern North America eastward across the Atlantic near 40^{o} N. Mean temperature differences between the positive and negative cases (Fig. 10e) exceed 8^{o} C over

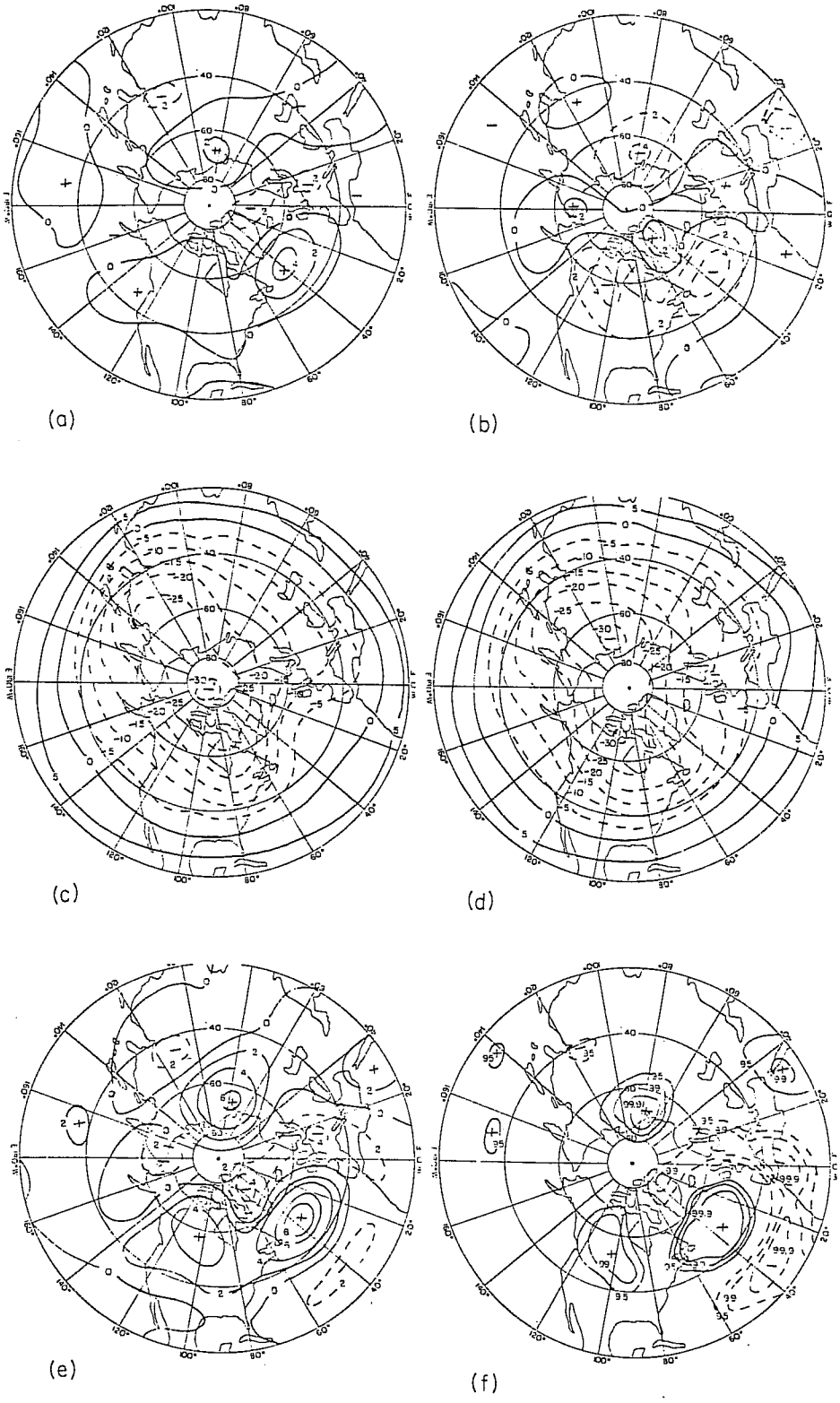

Fig. 10. As in Fig. 9 for composite 700 mb temperatures for the ATL cases (units: C)

the northern North Atlantic and are above 5^{o} C in several other regions, with temperatures in the positive cases greater (less) than those in the negative cases over virtually the entire North Atlantic north (south) of about 35^{o} N. The pattern of statistically significant differences (Fig. 10f) strongly resembles that obtained for the 500 mb height analyses, consistent with the observation that the tropospheric height and temperature anomaly patterns in these cases are highly positively correlated (Dole, 1986).

As may be anticipated from the previous analyses, the vorticity anomaly patterns at 300 mb (Figs. 11a and 11b) also closely resemble those seen in the height fields (aside, of course, from the sign changes), with peak vorticity anomalies having magnitudes of about $3 - 4 \times 10^{-5}$ sec $^{-1}$. The local minima in absolute vorticity associated with the positive height anomaly center (Fig.11c) has a value typical of air originating at subtropical latitudes (around 30^{o} N). In contrast, in the negative anomaly cases (Fig. 11d), the negative height anomalies over the eastern Atlantic are at one end of a band of high values of absolute vorticity that extends eastward over the northern North Atlantic from northeastern Canada, where climatological-mean values of absolute vorticity are high. Differences in the time-mean vorticity (Fig. 11e) have maximum values approaching 7×10^{-5} sec^{-1}, with much of the North Atlantic region displaying highly significant differences (Fig. 11f).

Similar analyses of an approximate form of the potential vorticity, $P = -(\zeta + f)\, g\, \partial\theta / \partial p$, where ζ is the relative vorticity evaluated on isobaric (250 mb and 300 mb) rather than isentropic surfaces, are not shown but display highly similar patterns, with the ridge in the positive cases associated with low values of potential vorticity typical of values seen the subtropics, and the negative height anomalies in the negative cases associated with high values of potential vorticity extending eastward from northern Canada.

Fig. 12 displays the corresponding composites of the rms bandpass 1000 mb heights, which have been used as in the previous section to estimate changes in synoptic-scale eddy activity.

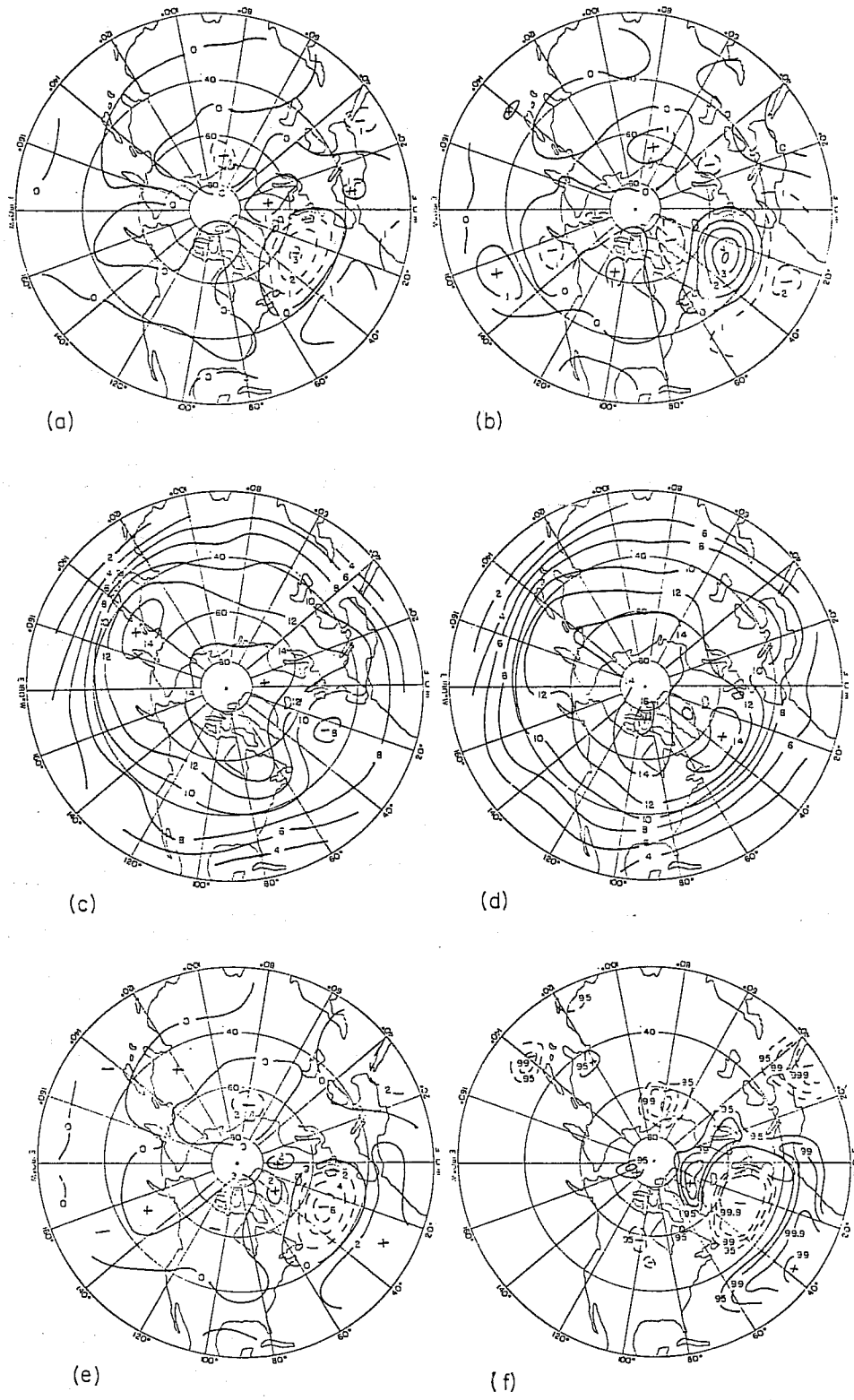

Fig. 11. As in Fig. 9 for 300 mb vorticity fields for the ATL cases (units: 10^{-5} sec^{-1}).

In the positive cases (Fig. 12a), a broad region of high variability extends northeastward from the eastern United States to Scandanavia, with primary maxima over the Canadian maritimes and to the east of Greenland. In contrast, the negative cases (Fig. 12b) display a single maximum located to the east of Newfoundland, with the axis of high variability extending along a more zonally-oriented band across most of the North Atlantic near 50^{o} N. Comparisons with the corresponding mean temperature analyses in Fig. 10 indicate that there is a good correspondence betwen the regions of maximum bandpass variability in the two cases and the regions of maximum baroclinity. The differences between means (Fig. 12c) and associated significance calculations (Fig. 12d) suggest that the significant changes are primarily associated with the more northward displacement of the storm paths in the positive cases, with a tendency in the positive cases for the variability to be relatively most strongly enhanced both to the west of Greenland and to the east of Greenland extending through Scandanavia, and most strongly suppressed over the central and eastern Atlantic.

Similar bandpass analyses (not shown) have been conducted for other levels (Dole, 1982; Dole, 1986). Many of the basic features in the 1000 mb analyses are also evident at the other levels; however, there is some indication that the portion of the storm path over the western Atlantic is relatively more prominent at low levels, while the storm path that extends from Greenland southeastward through Scandanavia toward the Black Sea continues to have a very strong signature at upper levels.

4.1.2. Differences in eddy terms in time-mean vorticity and heat budgets

In recent years there have been a growing number of time-mean budget studies that describe eddy activity in both climatological (see, e.g., Holopainen, 1983) and anomalous mean flows (e.g., Savijarvi, 1977, 1978; Dole, 1982; Illari, 1984; Trenberth, 1986a,b; Mullen, 1986; 1987; Holopainen and Fortelius, 1987). Here we briefly summarize a few of the results obtained from these analyses, first by examining differences in eddy terms in the

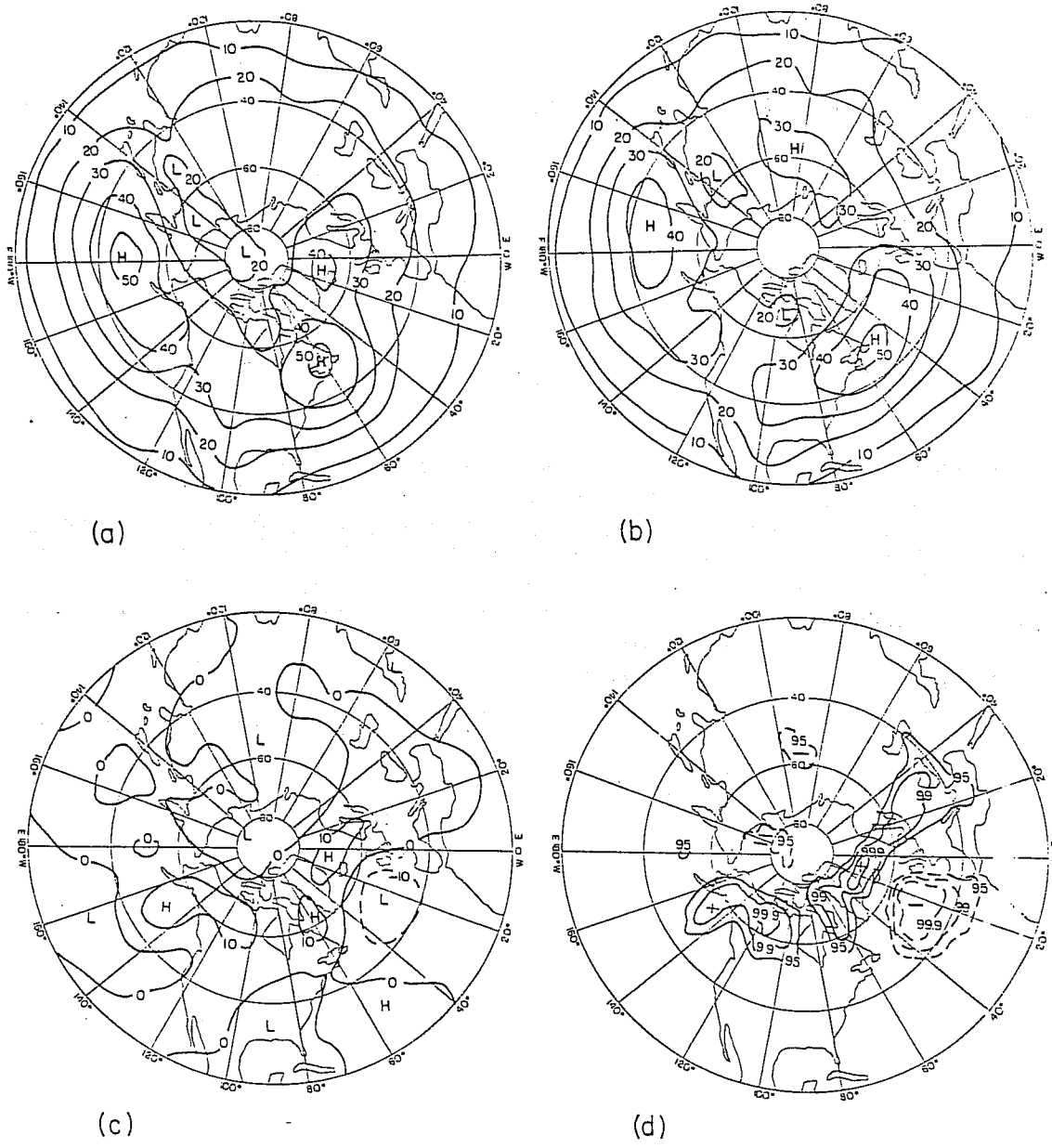

Fig. 12. Composite bandpass 1000 mb heights (units: m) for the (a) 12 ATL positive cases and (b) 12 ATL negative cases. (c) (Positive - negative) bandpass 1000 mb height differences (units: m). (d) Confidence levels for a two-sided t - test for the differences between mean values. Solid lines are positive differences as shown in (c), dashed lines are where the differences are negative.

time-mean thermodynamic and vorticity equations, and in the following section summarizing more recent results aimed at assessing the net effects of the eddies in time-mean budgets.

The isobaric coordinate form of the time-average thermodynamic equation may be written as

$$\overline{\frac{\partial \bar{T}}{\partial t}} = -\bar{\mathbf{V}} \cdot \nabla \bar{T} - \bar{\omega}\left(\frac{\partial \bar{T}}{\partial p} - \kappa \frac{\bar{T}}{p}\right) - \nabla \cdot \overline{\mathbf{V}'T'} - \left(\frac{\partial}{\partial p} - \frac{\kappa}{p}\right)\overline{\omega' T'} + \bar{Q} \qquad (1)$$

where the overbar represents a time-average over a case, a prime represents a deviation from that time average, and all other symbols have their usual meanings. This equation says that the local time-average temperature tendency may be expressed as the sum of four terms: the advection of the time-mean temperature by the time-mean flow, adiabatic cooling associated with time-mean vertical motions, horizontal eddy-heat flux convergence, adiabatic cooling associated with vertical eddy heat fluxes, and time-mean diabatic heating.

Similarly, the time-average vorticity equation may be written as

$$\overline{\frac{\partial \zeta}{\partial t}} = -\bar{\mathbf{V}} \cdot \nabla(\bar{\zeta} + f) - (\bar{\zeta} + f)\nabla \cdot \bar{\mathbf{V}} - \nabla \cdot \overline{\mathbf{V}'\zeta'} + \bar{F} + R_V \qquad (2)$$

where ζ is the relative vorticity, F represents sub-gridscale vorticity dissipation, and R_V is a residual term that includes contributions from vertical vorticity advection, vertical eddy vorticity flux convergence, and twisting terms. The first three terms on the right-hand side of (2) are the advection of time-mean absolute vorticity by the time-mean flow, the time-mean divergence term, and the horizontal vorticity flux convergence term. They contain

all of the terms present in the inviscid time-averaged quasi-geostrophic vorticity equation, as well as certain additional (usually smaller) terms (see, however, the recent discussion by Hoskins and Sardeshmuhk, 1987, on the possible importance of terms that have generally been assumed to be small in the mean vorticity balance). Scale analysis and observational data suggest that, at least in the free atmosphere at middle and high latitudes, the last two terms in (2) are also usually relatively small.

Most diagnostic analyses have focused primarily on the horizontal eddy flux divergence terms and, for brevity, we will do so here as well. Although both observational and theoretical results suggest that typical magnitudes of the vertical eddy flux terms are likely to be somewhat smaller than the horizontal flux terms, it is important to keep in mind that the effects of the vertical fluxes are by no means negligible and that, particularly in the thermodynamic balances, they play an important and systematic role.

Fig. 13 presents the composite mean 700 mb horizontal eddy heat flux convergence fields for the ATL cases. Comparison with the corresponding time-mean temperature analyses (Fig. 10) indicates that, as for the climatological-mean flow, the eddy flux convergence patterns for both the positive and negative cases are strongly negatively correlated with the temperature patterns, tending to produce cooling on the warm side of the region of maximum baroclinity and warming on the cold air side. The direct effect of the horizontal eddy heat fluxes is therefore to weaken the time-mean temperature anomalies; however, as we will discuss, vertical motions induced by the eddies will contribute to time-mean adiabatic temperature changes which partially oppose this direct effect. The general relationship seen in these cases between the mean temperature and horizontal heat flux convergence patterns is very robust. It is observed for both climatological (e.g., Holopainen,1970; Lau, 1979b) and anomalous mean flows (e.g., Savijarvi, 1977; Dole, 1982; Mullen, 1986), and is generally attributed to the pattern of downgradient heat fluxes associated with growing baroclinic waves in these regions.

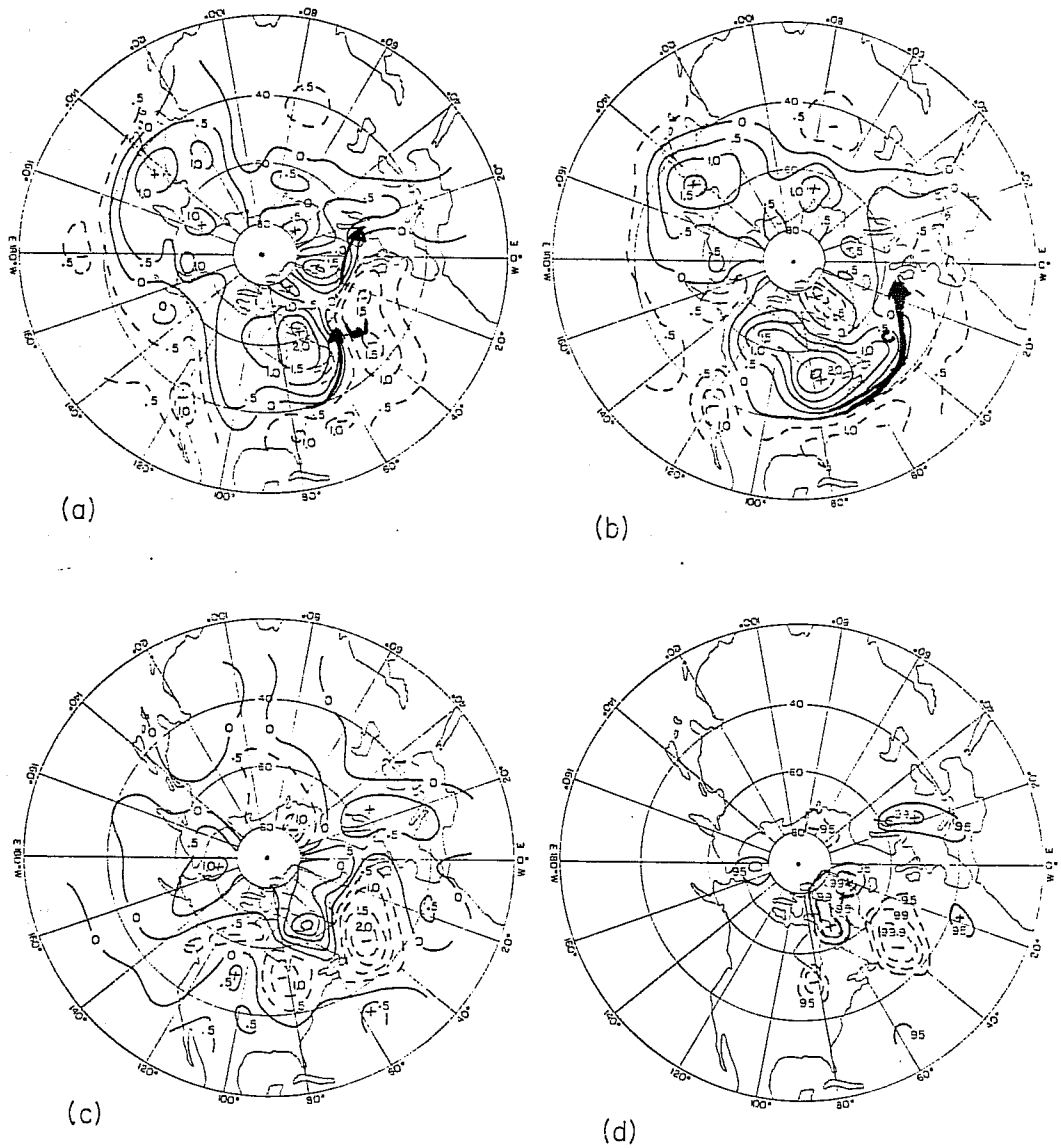

Fig. 13. As in Fig. 12 for the composite values of 700 mb eddy heat flux convergence (units: C d^{-1}) for the ATL cases.

Fig. 14 presents a similar analysis of the eddy vorticity flux convergence fields for the cases. Although the patterns are considerably noiser than in the corresponding eddy heat terms, careful comparison suggests that in both cases there is predominantly positive vorticity flux convergence on the poleward side and vorticity flux divergence on the equatorward side of the storm paths. The associated mean vorticity tendencies are generally to increase cyclonic vorticity on the cyclonic side and increase anticyclonic vorticity on the anticyclonic shear side of the jet stream. The eddy vorticity fluxes therefore contribute toward a tendency to increase the strength of the jet, similar to the effects of the momentum (and vorticity fluxes) determined in climatological budget studies (e.g., Blackmon, *et al.*, 1977; Holopainen, 1978; Lau, 1979b; Holopainen and Oort, 1981). Again, however, divergent circulations induced by the eddies will contribute to time-mean vorticity tendencies that will partially oppose this direct effect. The difference (Fig. 14c) and significance analyses (Fig. 14d) indicate, however, that only a small area near and upstream of the key region has differences exceeding the 99% confidence level. The low confidence values are a result of the strong case-to-case sampling variations that occur in the local values of this term. Indeed, the region of high significance is sufficiently small that it would fail to pass a global significance test (e.g., Livezey and Chen, 1983). From a purely statistical point of view, then, it would be difficult to reject the null hypothesis (of no significant differences between means).

Nevertheless, the vorticity flux convergence patterns in the vicinity of the persistent anomalies do bear some resemblance to the general patterns predicted in certain simple theories of eddy forcing of anomalous time-mean flows. In particular, in the positive anomaly cases (which are frequently associated with blocking), this term contributes to an anticyclonic vorticity tendency in the vicinity of and to the west of the anticyclonic vorticity center. Green (1977) originally proposed that anomalous upper-level eddy vorticity forcing could help to account for the persistence of blocking patterns; he suggested that, in order to

maintain the blocking against frictional dissipation, the vorticity forcing should be in-phase with the vorticity pattern. Austin (1980), however, presented a simple quasi-geostrophic analysis that suggested that at the wavelengths typical of blocking patterns, and assuming relatively weak dissipation, the upper-level eddy vorticity forcing should be approximately one quarter-wavelength upstream of the vorticity pattern, in order to balance the tendency for the block to be advected downstream by the time-mean flow. In numerical experiments with a barotropic model, Shutts (1983) also found that anticyclonic vorticity forcing on the western side of a blocking high tended to reinforce the blocking pattern.

Our results appear intermediate between the phase relationships predicted by Green (1977) and Austin (1980). Other time-mean budget studies, principally of blocking cases, have displayed a variety of phase relationships (or no relationships at all) between the eddy vorticity flux convergence patterns and the time-mean vorticity patterns. Illari (1984), Shutts (1986) and Mullen (1986), for example, find a tendency for the anticyclonic eddy forcing to be approximately a quarter-wavelength upstream of blocking highs, Holpainen and Fortelius (1987) suggest a more nearly in-phase relationship, while Savijarvi (1977) found no obvious phase relation (although the latter two studies are for individual cases). Some of these differences are undoubtedly due to sampling variations and to the intrinsic difficulty of getting reliable estimates from observations of such highly differentiated quantities; other differences are likely related to whether or not spatial or temporal filters have been applied to the data, as discussed by Mullen (1986). Comparisons with the other studies suggest that our results are probably most similar to those reported by Mullen (1986), who also conducted composite analyses for a relatively large number of both observed and model blocking cases in the Atlantic and Pacific regions.

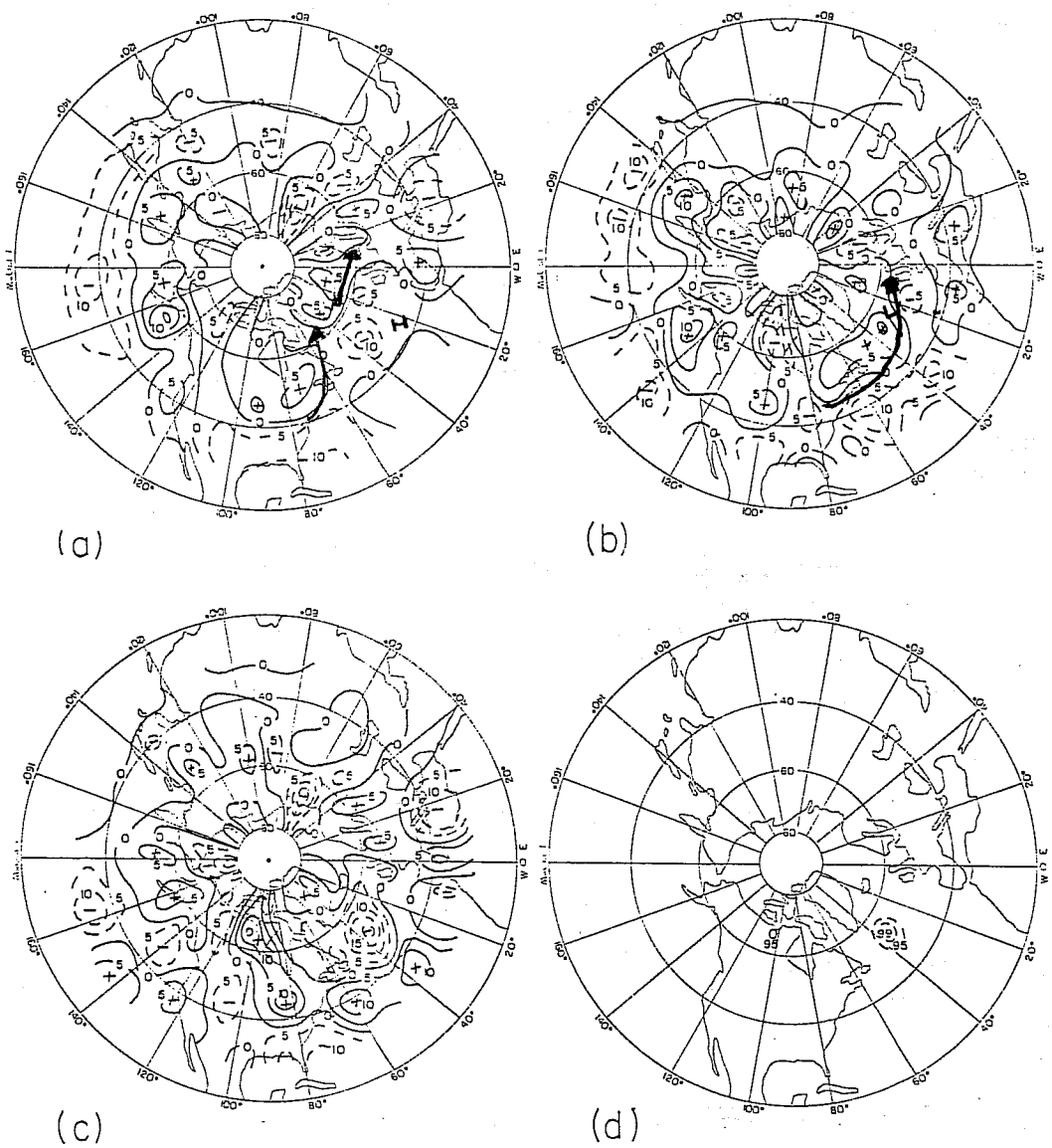

Fig. 14. As in Fig. 12 for the composite values of 300 mb eddy vorticity flux convergence (units: 10^{-12} s $^{-1}$) for the ATL cases.

4.1.3. Net effects of eddies inferred from time-mean budget analyses

In order to determine the net effects of the eddies on the mean flow, it is necessary to take into account the combined effects of the eddy flux convergences of vorticity and temperature and the eddy-induced mean secondary circulations. In recent years, a variety of approaches, generally based on the assumptions of quasi-geostrophic theory, have been developed to determine the net effects of transient eddies on time-mean three-dimensional flows (see, e.g., Holopainen and Fortelius, 1987).

In quasi-geostrophic theory (e.g., Hoskins, 1983), the net effect of transient eddies on the mean flow is given by the eddy flux convergence of quasi-geostrophic pseudopotential vorticity q in the interior of the fluid

$$\overline{\left(\frac{\partial q}{\partial t}\right)}_{TE} = - \nabla \cdot \overline{q'\mathbf{V}'} \qquad (3)$$

together with the eddy flux convergence of potential temperature θ at the lower and upper boundaries:

$$\overline{\left(\frac{\partial \theta}{\partial t}\right)}_{TE} = - \nabla \cdot \overline{\theta'\mathbf{V}'} \qquad (4)$$

From (3) together with the boundary conditions (4), a "tendency equation" for the time-mean geopotential height field can be obtained (Lau and Holopainen, 1984) that is analogous to the usual quasi-geostrophic geopotential tendency equation (e.g., Holton, 1979). For a quasi-geostrophic system, this equation gives the initial geopotential tendency that would be experienced for a specified forcing. Lau and Holopainen (1984) used this tendency method to examine the net effects of transient eddy heat and vorticity fluxes on the climatological mean wintertime flow. More recently, Mullen (1987) and Holopainen and Fortelius (1987) have performed similar calculations for blocking situations.

Fig. 15, from Mullen (1987), provides an illustration of this method for a composite of observed eastern Atlantic blocking cases. Figs 15a and 15b show, respectively, distributions of initial geopotential tendencies at 300 mb and 1000 mb associated with high-pass filtered transient eddy heat fluxes. We see that the tendencies at the two levels are essentially anti-phase, with the corresponding implied thickness tendencies being positive on the cold air side of the baroclinic zone and negative on the warm air side. As we would anticipate, then, the net effect of the heat fluxes is to reduce the baroclinity and therefore, through the thermal wind relation, to reduce the vertical shear in this region, with the changes in thermal wind accomplished through Coriolis torques acting on the associated mean ageostrophic circulation.

Figs. 15c and 15d show similar analyses for the effects of the high-pass filtered transient eddy vorticity fluxes. The implied geopotential tendencies are nearly in-phase at both levels, with the positive tendencies near and upstream of the blocking anticyclone associated with the maxima in vorticitity flux divergence in this region (cf. Fig. 13). In these cases, the net tendency patterns at both 300 mb (Fig. 15e) and 1000 mb (Fig. 15f) roughly resemble the patterns implied by the vorticity forcing, with positive tendencies located near and upstream of the blocked region at both levels.

4.2. Effects of Eddies Inferred from "Extended" Eliassen-Palm Fluxes

An alternative approach for assessing the net effects of eddies is based essentially on attempts to develop extensions for time-mean flows of diagnostic analyses of wave-mean flow interactions deduced from Eliassen-Palm fluxes (Hoskins *et al.*, 1983; Plumb, 1985, 1986; Trenberth, 1986b). For zonal-mean flows, the Eliassen-Palm (E-P) flux provides an indication of both the flux of eddy activity and the net eddy forcing of the zonal mean flow (Andrews and McIntyre, 1976; Edmon *et al.*, 1980). Although the corresponding theory for

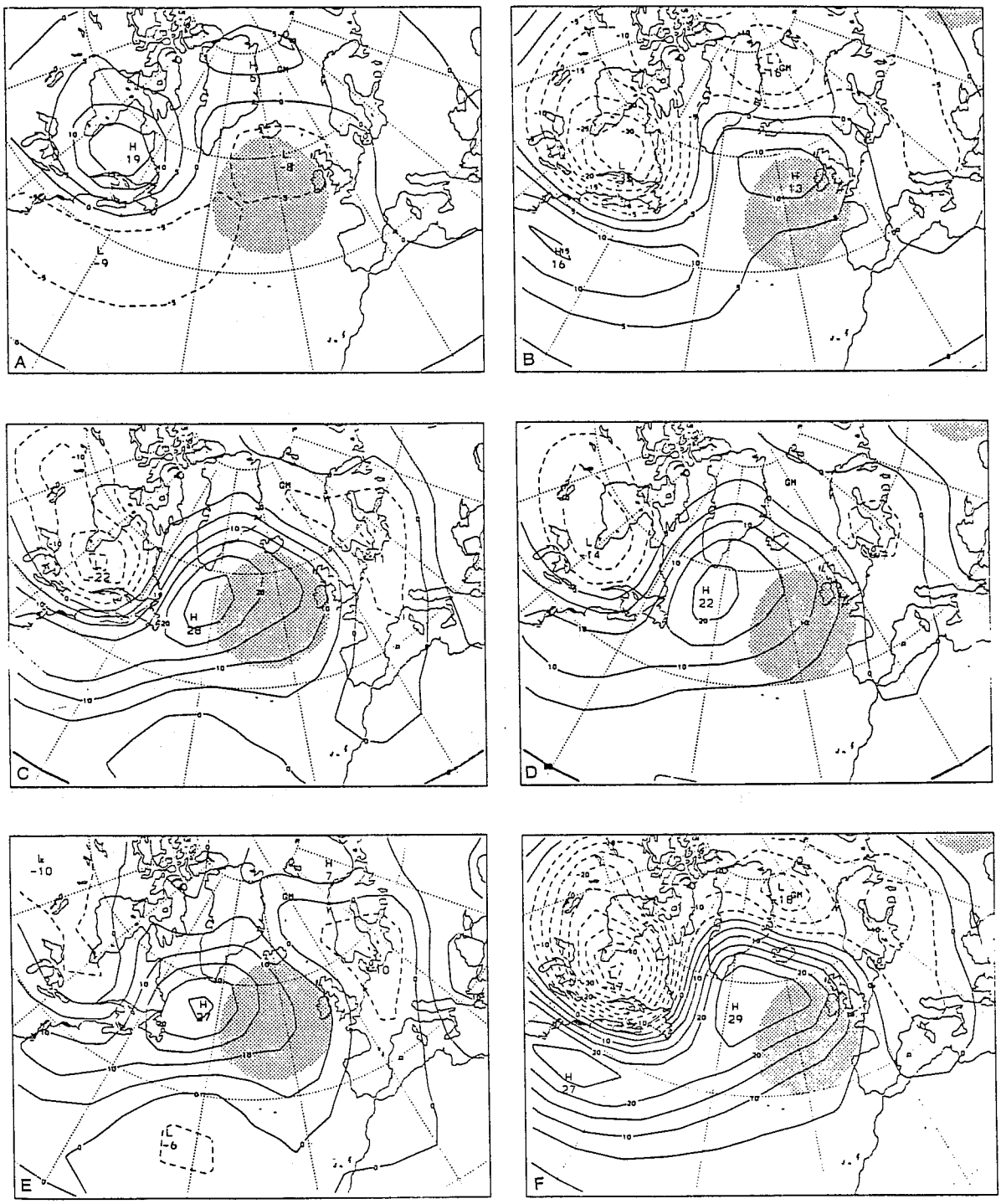

Fig. 15.

Distributions of the geopotential tendencies associated with transient eddy heat fluxes at (a) 300 and (b) 1000 mb, with transient eddy vorticity fluxes at (c) 300 and (d) 1000 mb, and with transient eddy heat and vorticity fluxes at (e) 300 and (f) 1000 mb for observed Atlantic blocking composite. Eddy forcings are computed using highpass filtered data. Contour interval is 5.0 × 10^{-4} m^2 s^{-3}, negative contours are dashed. In (a), (c), and (e), stippling denotes regions where the departure of time-mean geopotential height from the zonal average $\bar{Z}^*$ at 300 mb exceeds 300 m; in (b), (d), and (f), stippling denotes regions where $\bar{Z}^*$ at 1000 mb exceeds 50 m.

(From Mullen, 1987)

time-mean flows is less well-developed, some of the results that have been obtained in initial observational applications are quite intriguing, and provide indications of processes that may be quite important in anomalous large-scale flows such as blocking. As the theory is still in its early stages, a variety of different formulations of these fluxes have been proposed (for a review and discussion of the relative merits of some of the different formulations, see Trenberth, 1986b); here, however, we will illustrate a few results obtained from the "E-vector method" of Hoskins *et al.* (1983).

In pressure coordinates, the components of the three-dimensional "**E**-vector" of Hoskins *et al.* (1983) are given by

$$\mathbf{E} = \left(v'^2 - u'^2 \, , \; - u' v' \, , \; f_o \frac{\overline{v'\theta'}}{\Theta_p} \right) \qquad (5)$$

where the primed quantities denote departures from the climatological-mean values and Θ_p is the vertical (pressure) derivative of the horizontally and temporally averaged static stability. The directions and magnitudes of the **E**-vectors can be seen to be related to important aspects of the local structures of the eddies. The x-component of **E**, for example, is related to asymmetries in the shapes of the disturbances, with positive values associated with meridionally elongated eddies (i.e., having $v'^2 > u'^2$) and negative values associated with zonally elongated eddies ($v'^2 < u'^2$); the y-component to horizontal phase tilts, with positive values associated with phase lines that slope toward the west with increasing latitude (e.g., northwest - southeast tilted ridges and troughs), and negative values with phase lines that slope toward the west with decreasing latitude (northeast-southwest tilted ridges and troughs); and the vertical component to vertical phase tilts, with positive values for disturbances that have phase lines that slope toward the west with increasing height.

Hoskins *et al.* show that, subject to certain approximations, the acceleration of the mean westerly flow by the transient eddies is given by $\nabla \bullet \mathbf{E}$, and in particular, where

$\nabla \bullet \mathbf{E} > 0$, there is a net forcing by the eddies consistent with a tendency to increase the westerly component of the mean flow. As a simple example, consider the case of growing baroclinic waves in the early stages of the their evolutions as, for example, in the storm path entrance regions. These disturbances are associated with downgradient (essentially poleward) directed heat fluxes in the troposphere, with largest magnitudes typically between 850 mb and 700 mb. From (5) , the corresponding **E** - vectors have upward-directed components that typically peak in the lower to mid-troposphere. Typically, then, at low levels in these regions $\nabla \bullet \mathbf{E} > 0$, while in the upper troposphere $\nabla \bullet \mathbf{E} < 0$. The eddies therefore contribute to a tendency for the mean westerly flow to increase at low levels and to decrease in the upper troposphere; that is, they tend to reduce the mean westerly shear, as we would anticipate.

Hoskins *et al.* (1983), Shutts (1986) and (with a slightly different formulation) Trenberth (1986b) present **E** - vector patterns associated with blocking cases; Fig. 16 (from Shutts, 1986) displays one example of (two-dimensional) **E** - vector patterns for a case of blocking over the Atlantic. In this analysis, the **E** - vectors have been obtained from 300 mb data that have been high-pass filtered (retaining periods of approximately 7 days or less). We see that, well-upstream of the blocked region, the **E** - vectors are mainly directed eastward, indicative of eddies that are primarily meridionally elongated. As the eddies approach the region where the large-scale flow becomes strongly diffluent, the magnitudes of the **E** - vectors typically first increase, and then become very small. The initial increase is the manifestation of a tendency for the eddies to reduce their zonal wavelengths and become markedly stretched meridionally (with corresponding increases in the values of $(v'^2 - u'^2)$ as they enter the region where the mean zonal flow is decreasing rapidly downstream; the smaller magnitudes are associated with the very low values of high-pass variance observed in the vicinity of the blocking anticyclone (as seen also in the previous section). Shutts (1986) has suggested that these **E** - vector patterns are the signature of an essentially barotropic "eddy - straining" mechanism that results in the collapse of the

east-west scale of the eddies as they enter the diffluent flow region upstream of the block.

The variations in the eddies as they approach the block result in a convergence of $\mathbf{E}$ - vectors near and just to the south of the anticyclonic vorticity center, implying a tendency to further decrease the strength of the mean westerly flow in a region where it is already weak. In addition, there is a "fanning out" of E - vectors (essentially a manifestation of "bowed" troughs and ridges) in the westerlies well the south of the anticyclone so that $\nabla \bullet \mathbf{E} > 0$, implying a tendency for the eddies to increase the strength of the mean westerlies in the region where the westerlies are already anomalously strong. An additional region where $\nabla \bullet \mathbf{E} > 0$ is located in the westerlies to the north of the blocking anticyclone. These analyses suggest, then, that not only may the large-scale flow anomalies that are associated with blocking lead to changes in synoptic-scale eddy activity, but also that the changes in eddy activity may result in a net forcing on the mean flow that tends to maintain or intensify the large-scale flow anomalies.

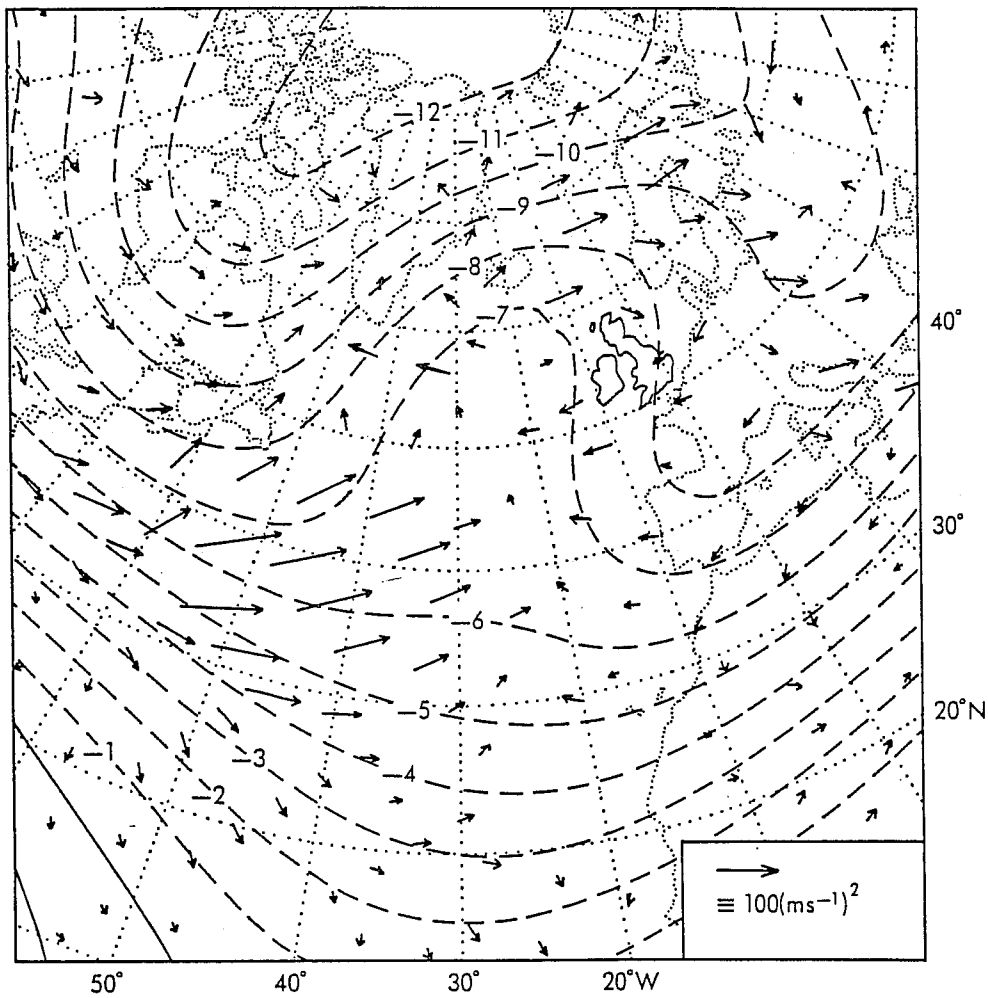

Fig. 16. High-pass filtered E vectors superimposed on the mean streamfunction field for a case of blocking over the North Atlantic (from Shutts, 1986).

5. DISCUSSION

We have attempted to identify systematic relationships between variations in synoptic-scale eddy activity and persistent large-scale flow anomalies. We focused first on determining how synoptic-scale eddy activity varies for the widely-differing large-scale flows, and then on how the changes in the synoptic-scale eddies may influence the large-scale flow anomalies.

In comparing situations characterized by widely-differing large-scale flows, we found corresponding well-defined differences in synoptic-scale eddy activity. To a considerable extent, the observed differences in eddy activity conform with synoptic experience and with simple theoretical expectations. In general, in both positive anomaly and negative anomaly cases, the storm paths approximately coincide with the zones of maximum time-mean baroclinity. Enhanced variability also tends to occur near and to the east side of the major long wave troughs and, conversely, variability is usually markedly suppressed near and to the east of major long wave ridges.

In addition, there were clear indications of orographic influences on the variations in eddy activity, with variability typically being enhanced on the lee sides of major mountain barriers in regions of stronger than normal flow. One manifestation of the orographic influences was the appearance of "secondary" genesis regions (to the lee of the U.S. Rockies in the PAC positive cases and the Canadian Rockies in the PAC negative cases, and to the lee of Greenland in the ATL positive cases) in addition to the "primary" regions in the eastern continent - western ocean regions found in climatological analyses (e.g., Blackmon *et al.*, 1977). Indeed, in the climatological analyses, direct orographic influences appear almost suprisingly absent, with only weak indications of enhanced variability appearing on the lee sides of major mountain barriers. The present results hint at a possible explanation for this relatively weak signature: "lee cyclogenesis" may depend rather sensitively on the character

of the large-scale flow, so that the occurrence and favored locations of this form of cyclogenesis may vary considerably for different large-scale flows. In comparison, it seems likely that the primary genesis regions may depend relatively less on the details of the large-scale flow, but are instead geographically fixed by the semi-permanent zones of strong baroclinity that are located in wintertime over the eastern continent - western ocean regions.

We also presented some results of studies on the relationships of variations in cyclogenesis to persistent anomalies in surface temperatures. Although the results are preliminary, they did provide indications that significant variations in the deepening rates of cyclones were associated with the temperature anomalies. Although some of the differences between warm and cold events are likely to be attributable to corresponding changes in the mean long wave patterns, it seems quite plausible that variations in surface baroclinity and low-level static stability also play significant roles.

We then turned to the problem of how changes in synoptic-scale eddy activity may influence the large-scale flow. In examining time-mean budgets of heat and vorticity, we were able to identify significant and well-defined differences in eddy terms in the heat budgets, but fewer significant differences in the corresponding vorticity budget terms. This is undoubtedly partly due to the greater sensitivity of the vorticity calculations to analysis errors, but may also reflect the relatively less systematic character of eddy momentum fluxes compared with eddy heat fluxes in baroclinic waves, as discussed, for example, by Hoskins (1978) and Held and Andrews (1983). Many of the systematic changes that we have identified appear qualitatively consistent with the changes expected for baroclinic waves that are evolving on a spatially-varying mean flow (e.g., Pierrehumbert, 1986).

Although the eddy vorticity terms displayed few statistically significant differences between positive anomaly and negative anomaly cases, there were nevertheless a number of intriguing similarities to results predicted in simple theories on the role of eddies in forcing large-scale circulation anomalies (e.g., Green, 1977; Austin, 1980; Shutts, 1983, 1986; Haines and

Marshall, 1987). In addition to our results, studies of the net forcings of anomalous mean flows by eddies as deduced from tendency methods (e.g., Holopainen and Fortelius, 1987; Mullen, 1987) and E - vector analyses (Hoskins et al., 1983; Shutts, 1986; Trenberth, 1986b) have shown substantial evidence that eddies play an important role in maintaining certain anomalous flow patterns such as blocking. The results of the E-vector analyses are particularly interesting in this regard, as they suggest that not only may the large-scale flow variations lead to modifications in the structure and behavior of the synoptic-scale eddies, but also that the changes in the eddies may result in a net forcing on the mean flow that tends to reinforce the pre-existing large-scale flow anomalies.

Aside from the direct effects of the eddy fluxes, indirect effects of the synoptic-scale eddies may also have important influences on the large-scale flow. More complete budget analyses (e.g., Dole, 1982), for example, indicate that changes in the time-mean diabatic heating between positive and negative anomaly cases are closely related to the changes in storm paths, primarily through changes in latent (but also sensible and radiative) heating patterns. The relationships between latent, sensible and radiative heating patterns and storm paths are poorly understood, but are certainly at least partly geographically dependent. To the extent that the synoptic-scale eddies influence the zonal-mean flow, they may also indirectly alter the generation and propagation characteristics of planetary scale waves.

In addition, as Held and Hoskins (1985) have stressed, the effects of eddies may be markedly non-local, so that the observed mean-flow tendencies due to eddy fluxes can be misleading. Conceivably, for example, eddy - mean flow interactions might occur until the flow approaches a "quasi-equilibrium" where the interactions appear small, suggesting that the eddies may be neglected. The quasi-equilibrium flow, however, need bear no obvious relation to any equilibria calculated by neglecting the eddies. Reinhold and Pierrehumbert (1982) find such a behavior in a low-order model.

Indeed, even the sign of the eddy forcing may not be indicative of the role of the eddies.

Held *et al.* (1986) , for example, demonstrate how in some situations, synoptic-scale eddies can increase the amplitudes of planetary waves by catalyzing the release of zonal - mean available potential energy, even though a diagnostic analysis of the direct effects of the eddy heat fluxes would suggest that the eddies are playing a dissipative role.

The present examples are not meant to minimize the importance of diagnostic analyses, but only to emphasize that interpretations of their results are often suprisingly subtle. In particular, causality may be difficult (if not impossible) to infer from time-mean budget analyses alone. It seems likely that the clearest results on causal relationships will come from careful studies of the time evolution of particular events that are done in conjunction with simple modelling studies; studies considering the time evolution of potential vorticity may be particularly useful in this regard (recent examples are given in Hoskins *et al.*, 1985 and Shutts, 1986). Nevertheless, based on current results, it does seem likely that, in the development and maintenance of certain anomalous large scale flows such as blocking, synoptic-scale eddies often do play a crucial role.

The current results, then, once again present a picture of the rich interplay between synoptic-scale eddies and the large-scale flow on which they evolve. From an operational standpoint, the present results suggest that the failure to adequately simulate the large-scale flow will result in errors in predicting the regions of cyclogenesis and subsequent storm paths; however, the results also suggest that deficiencies in predicting the synoptic-scale eddies may contribute significantly to errors in forecasting the large-scale flow.

Acknowledgments

Much of the work for section 3 is part of joint research efforts on cyclogenesis with graduate students Mr. Peter Neilley and Mr. Bradford Lyon, and I am particularly grateful for their assistance in preparing material used in the presentation. I also thank the American Meteorological Society and Academic Press for their permission to reproduce figures from work by Drs. S. Mullen and G. Shutts within the lecture notes. Ms. Isabelle Kole expertly drafted several of the figures. Some of the calculations were performed on the Goddard Space Flight Center computer system located at Greenbelt, Maryland; the remainder were performed at MIT or on the National Center for Atmospheric Research computer system. NCAR is supported by the National Science Foundation. Support for this research was provided by NASA grants NASA-g NAGw-525 and NASA-g NAG5-927.

References

Andrews, D. G., and M. E. McIntyre, 1976: Planetary waves in horizontal and vertical shear: The generalized Eliassen-Palm relation and the mean zonal acceleration. *J. Atmos. Sci.,* **33,** 2031 - 2048.

Austin, J. F., 1980: The blocking of middle latitude westerly winds by planetary scale waves. *Q. J. R. Meteorol.. Soc.,* **106,** 327 - 350.

Berggren, R., B. Bolin, and C. G. Rossby, 1949: An aerological study of zonal motion, its perturbation and breakdown. *Tellus,* **1,** 14 - 37.

Blackmon, M. L. 1976: A climatological spectral study of the geopotential height of the Northern Hemisphere. *J. Atmos. Sci.,* **33,** 1607 - 1623.

_____, J. M. Wallace, N.C. Lau, and S. L. Mullen, 1977: An observational study of the Northern Hemisphere wintertime circulation. *J. Atmos. Sci.,* **34,** 1040 - 1053.

Colucci, S. J., 1985: Explosive cyclogenesis and large-scale circulation changes: Implications for atmospheric blocking. *J. Atmos. Sci.,* **42,** 2701-2717.

_____, 1987: Comparative diagnosis of blocking versus non-blocking planetary-scale circulation changes during synoptic-scale cyclogenesis. *J. Atmos. Sci.,* **44,** 125-139.

Dole, R. M., 1982: *Persistent anomalies of the extratropical Northern Hemisphere wintertime circulation.* Ph.D. thesis, Massachusetts Institute of Technology, Cambridge, Mass. 02139. Thesis available from the author on request.

_____, 1986a: Persistent anomalies of the extratropical Northern Hemisphere wintertime circulation: Structure. *Mon. Weather Rev.,* **114,** 178-207.

_____, 1986b: The life cycles of persistent anomalies and blocking over the North Pacific. *Adv. in Geophysics* , **29,** 31-69.

Edmon, H. J., B. J. Hoskins and M. E. McIntyre, 1980: Eliassen-Palm cross sections for the troposphere. *J. Atmos. Sci.,* **37,** 2600-2616.

Egger, J., 1978: Dynamics of blocking highs. *J. Atmos. Sci.,* **35,** 1788-1801.

_____, W. Metz and G. Muller, 1986: Forcing of planetary-scale blocking anticyclones by synoptic-scale eddies. *Adv. in Geophysics* , **29,** 183-198.

Frederiksen, J. S., 1979: The effect of long planetary waves on regions of cyclogenesis: Linear theory. *J. Atmos. Sci.,* **36,** 195-204.

_____, 1982: A unified three-dimensional instability theory of the onset of blocking and cyclogenesis. *J. Atmos. Sci.,* **39,** 967-987.

_____, 1983: A unified three-dimensional instability theory of the onset of blocking and cyclogenesis. II. Teleconnection patterns. *J. Atmos. Sci.,* **40,** 2593-2609.

_____, 1986: Instability theory and nonlinear evolution of blocks and mature anomalies. *Adv. in Geophysics,* **29,** 277-303.

Gall, R., R. Blakeslee and R. Sommerville, 1979: Cyclone-scale forcing of long waves. *J. Atmos. Sci.,* **36,** 1692-1698.

Green, J. S. A., 1977: The weather during July 1976: Some dynamical considerations of the drought. *Weather,* **32**, 120-128.

Haines, K., and J. Marshall, 1987: Eddy-forced coherent structures as a prototype of atmospheric blocking. *Quart. J. Roy. Met. Soc.,* **113,** 681-704.

Hansen, A. R., and T. C. Chen, 1982: A spectral energetics analysis of atmospheric blocking. *Mon. Weather Rev.,* **110,** 1146-1165.

_____, and A. Sutera, 1984: A comparison of the spectral energy and enstrophy budgerts of blocking versus nonblocking periods. *Tellus,* **36A,** 52-63.

Held, I. M., 1983: Stationary and quasi-stationary eddies in the extratropical troposphere: theory. In: Large-scale Dynamical Processes in the Atmosphere, B. J. Hoskins and R. P. Pearce, eds., Academic Press, London, p. 127-168.

_____, and D. G. Andrews, 1983: On the direction of eddy momentum flux in baroclinic instability. *J. Atmos. Sci.,* **40,** 2220 - 2231.

_____ , and B. J. Hoskins, 1985: Large-scale eddies and the general circulation of the troposphere. *Adv. in Geophysics,* **28A,** 3 - 32.

_____, R. T. Pierrehumbert and R. L. Panetta, 1986: Dissipative destablization of external Rossby waves. *J. Atmos. Sci.,* **43,** 388-396.

Holopainen, E., 1970: An observational study of the energy balance of the stationary disturbances in the atmosphere. *Quart. J. Roy. Met. Soc.,* **96**, 626-644.

_____ , 1978: On the dynamic forcing of the long-term mean flow by the large-scale Reynolds' stresses in the atmosphere. *J. Atmos. Sci.,* **35**, 1596-1604.

_____ , 1983: Transient eddies in midlatitudes: Observations and interpretation. In *Large-Scale Dynamical Processes in the Atmosphere* (B. J. Hoskins and R. P. Pearce, eds.), Academic Press, London, p. 201-234.

_____ , and A. H. Oort, 1981: On the role of large-scale transient eddies in the maintenance of the vorticity and enstrophy of the time mean atmospheric flow. *J. Atmos. Sci.,* **38**, 270-280.

_____ , and C. Fortelius, 1987: High-frequency transient eddies and blocking. *J. Atmos. Sci.,* **44,** 1632-1645.

Holton, J., 1979: An Introduction to Dynamic Meteorology. Academic Press, New York, N. Y.

Hoskins, B. J., 1978: Linear and nonlinear baroclinic instability on a sphere. In: The General Circulation: Theory, modeling and observations. NCAR Summer Colloquium, 1978. Boulder, CO. p. 116 - 143.

Hoskins, B. J., 1983: Modeling of the transient eddies and their feedback on the mean flow. In Large-Scale Dynamical Processes in the Atmosphere (B. J. Hoskins and R. P. Pearce, eds.), Academic Press, p. 169-199.

_____ , I. N. James, and G. H. White, 1983: The shape, propagation and mean-flow interaction of large-scale weather systems. *J. Atmos. Sci.,* **40,** 1595-1612.

_____, M. E. McIntyre and A. W. Robertson, 1985: On the use and significance of isentropic potential vorticity maps. *Quart. J. Roy. Met. Soc.*, **111**, 877-946.

_____, and P. D. Sardeshumkh, 1987: Transient eddies and the seasonal mean rotational flow. *J. Atmos. Sci.*, **44**, 328 - 338.

Illari, L., 1984: A diagnostic study of the potential vorticity in a warm blocking anticyclone. *J. Atmos. Sci.*, **41**, 3518-3526.

_____, and J.C. Marshall, 1983: On the interpretation of eddy fluxes during a blocking episode. *J. Atmos. Sci.*, **40**, 2232-2242.

Kalnay-Rivas, E. and L. O. Merkine, 1981: A simple mechanism for blocking. *J. Atmos. Sci.*, **38**, 2077-2091.

Lau, N.- C., 1978: On the three dimensional structure of the observed transient eddy statistics of the Northern Hemisphere wintertime circulation. *J. Atmos. Sci.*, **35**, 1900-1923.

_____, 1979a: The structure and energetics of transient disturbances in the Northern Hemisphere wintertime circulation. *J. Atmos. Sci.*, **36**, 982-995.

_____, 1979b: The observed structure of tropospheric stationary waves and local balances of vorticity and heat. *J. Atmos. Sci.*, **36**, 996-1016.

_____, and E. O. Holopainen, 1984: Transient eddy forcing of the time-mean flow as identified by geopotential tendencies. *J. Atmos. Sci.*, **41**, 313-328.

Livezey, R. E., and W. Y. Chen, 1983: Statistical field significance and its determination by Monte Carlo techniques. *Mon. Wea. Rev.*, **111**, 46 - 59.

Malanotte-Rizzoli, P. and P. Malguzzi, 1987: Coherent structures in a baroclinic atmosphere. Part III: Block formation and eddy forcing. *J. Atmos. Sci.*, **44**, 2493 - 2505.

Metz, W., 1987: Transient eddy forcing of low-frequency atmospheric variability. *J. Atmos. Sci.*, **44**, 2407 - 2417.

Mullen, S. L., 1986: The local balances of vorticity and heat for blocking anticyclones in a spectral general circulation model. *J. Atmos. Sci.*, **43**, 1406 - 1441.

_____, 1987: Transient eddy forcing of blocking flows. *J. Atmos. Sci.*, **44**, 3-22.

Palmen, E., and C. Newton, 1969: *Atmospheric Circulation Systems: Their Structure and Physical Interpretation.* Academic Press, New York, N.Y., 603 pp.

Petterssen, S., 1955: A general survey of the factors influencing development at sea level. *J. Meteor.*, **12**, 36-42.

_____, 1956: *Weather Analysis and Forecasting*, Vol. 1. Mcgraw-Hill, New York, N. Y.

Pierrehumbert, R. T., 1986: The effect of local baroclinic instability on zonal inhomogeneities of vorticity and temperature. *Adv. in Geophysics* , **29**, 165 - 182.

Plumb, R. A., 1985: On the three-dimensional propagation of stationary waves. *J. Atmos. Sci.*, **42**, 217-229.

_____, 1986: Three-dimensional propagation of transient quasigeostrphic eddies and its relationship with the eddy forcing of the time-mean flow. *J. Atmos. Sci.*, **43**, 1657-1678.

Reinhold, B. B. and R. T. Pierrehumbert, 1982: Dynamics of weather regimes: Quasi-stationary waves and blocking. *Mon. Weather Rev.*, **110**, 1105-1145.

Rex, D. P., 1950a: Blocking action in the middle troposphere and its effects on regional climate. I. An aerological study of blocking. *Tellus*, **2**, 196-211.

_____, 1950b: Blocking action in the middle troposphere and its effects on regional climate. II. The climatology of blocking action. *Tellus*, **2**, 275-301.

_____, 1951: The effect of Atlantic blocking action upon European climate.*Tellus*, **3**, 1-16.

Sanders, F. and J. G. Gyakum, 1980: The synoptic-dynamic climatology of the bomb. *Mon. Weather Rev.*, **108**, 1589-1606.

Savijarvi, H., 1977: The interaction of the monthly mean flow and large-scale transient eddies in two different circulation types. Part II: Vorticity and temperature balance. *Geophysica*, **14**, 207-229.

_____, 1978: The interaction of the monthly mean flow and large-scale transient eddies in two different circulation types. Part III: Potential vorticity balance. *Geophysica*, **15**, 1-16.

Shutts, G. J., 1983: The propagation of eddies in diffluent jet streams: eddy vorticity forcing of blocking flow fields. *Q. J. R. Meteorol. Soc.*, **109**, 737-761.

_____, 1986: A case study of eddy forcing during an Atlantic blocking episode. *Adv. in Geophysics*, **29**, 135 - 164.

Simmons, A. J., and B. J. Hoskins, 1978: The life cycles of some nonlinear baroclinic waves. *J. Atmos. Sci.*, **35**, 414-432.

_____, 1980: Barotropic influences on the growth and decay of nonlinear baroclinic waves. *J. Atmos. Sci.*, **37**, 1679-1684.

Trenberth, K. E., 1986a: The signature of a blocking episode on the general circulation in the Southern Hemisphere. *J. Atmos. Sci.*, **43**, 2061-2069.

_____, 1986b: An assesment of the impact of transient eddies on the zonal flow during a blocking episode using localized Eliassen-Palm flux diagnostics. *J. Atmos. Sci.*, **43**, 2070-2087.

Wallace, J. M., and Gutzler, D. S., 1981: Teleconnections in the geopotential height field during the Northern Hemisphere winter. *Mon. Weather Rev.*, **109**, 784-812.

White, W.B. and N. E. Clark, 1975: On the development of blocking ridge activity over the central North Pacific. *J. Atmos. Sci.*, **32**, 489-502.